THERMAL REMOVAL OF MERCURY FROM SPENT POWDERED ACTIVATED CARBON (PAC) SORBENT IN COAL-FIRED ELECTRIC POWER PLANTS

by

George D.O. Okwadha

A Thesis Submitted in
Partial Fulfillment of the
Requirements for the Degree of

Master of Science
in Engineering

at

The University of Wisconsin-Milwaukee
December 2006

THERMAL REMOVAL OF MERCURY FROM SPENT POWDERED ACTIVATED CARBON (PAC) SORBENT IN COAL-FIRED ELECTRIC POWER PLANTS

by

George D.O. Okwadha

A Thesis Submitted in
Partial Fulfillment of the
Requirements for the Degree of

Master of Science
in Engineering

at

The University of Wisconsin-Milwaukee
December 2006

Major Professor

Graduate School Approval

ABSTRACT

THERMAL REMOVAL OF MERCURY FROM SPENT POWDERED ACTIVATED CARBON (PAC) SORBENT IN COAL-FIRED ELECTRIC POWER PLANTS

by

George D.O. Okwadha

The University of Wisconsin-Milwaukee, 2006
Under Supervision of Dr. Jin Li

The US Environmental Protection Agency (EPA) issued the first ever federal rule to permanently cap and reduce mercury emissions from coal-fired power plants on March 15, 2005. The rule referred to as The Clean Air Mercury Rule (CAMR) when fully implemented, will reduce utility emissions of mercury from 48 tons a year to 15 tons by 2018, a reduction of nearly 70%. These mandatory declining caps coupled with significant penalties for noncompliance, will ensure that mercury reduction requirements are achieved and sustained.

In anticipation of this rule, scientists and organizations in collaboration with EPA and US Department of Energy (DOE) are carrying out research to understand the science of mercury speciation, and its fate and transport within the atmosphere, in order to develop more efficient and cost-effective mercury control technologies and devices.

This research develops and demonstrates a technology to liberate mercury adsorbed onto powdered activated carbon (PAC) sorbent by the TOXECON^{TM} process, and recommends further evaluation of the regenerated PAC. The TOXECON^{TM} process is the patent of Electric Power Research Institute (EPRI). It involves injecting activated carbon downstream of an existing primary particulate control device and upstream of a

second particulate control device. The pilot scale (Air Scale) apparatus removed 65%, 83% and 92% of mercury without addition of catalysts when run at 900^{o}F, 1000^{o}F, and 1100^{o}F respectively at a constant rotary feed speed of 1200 rpm. The experimental results indicate that elemental mercury can be removed using the pilot scale (Air Slide) apparatus with reasonable efficiency. The bench scale experiment using thermogravimetric analyzer (TGA) removed 29%, 100%, 100%, and 100% at operation temperatures of 800^{o}F, 900^{o}F, 1000^{o}F, and 1100^{o}F respectively without catalysts, and 100% mercury removal with catalysts at 700^{o}F and beyond. This bench scale result demonstrates that mercury can be liberated with a higher efficiency in a controlled environment. It also demonstrates that a mixture of 1% copper (II) oxide (CuO) and 4% Iron (III) oxide (Fe_2O_3) catalyst, and 5% cuprous chloride can enhance mercury liberation at lower temperatures in the bench scale (TGA) experiments. The catalytic performance of 5% cuprous chloride (CuCl) was identical to that of the copper-iron mixture. Carbon loss as determined by loss on ignition (LOI) was minimal, but increased with temperature to a maximum of about 13% with and without catalysts. Scanning electron microscope (SEM) analysis on the PAC samples from the TOXECON^{TM} process observed no change in particle aggregation. However, particles from the pilot scale apparatus baghouse looked finer than the rest. In general, thermal treatment had no effect on particle morphology. Energy Dispersive X-ray (EDX) analysis shows the PAC sample from the TOXECON^{TM} process is composed of coarse and fine particles. The coarse particles were rich in calcium and sulfur embedded in a matrix of carbon; whereas the fines were fly ash particles rich in aluminum, silicon and magnesium. The chemistry of the PAC samples from the TOXECON^{TM} process was the same in all the samples examined. Moreover, the

adsorption capacity of the regenerated PAC is not expected to be substantially affected by thermal treatment because there was only 13% carbon loss with little or no aggregation of the particles.

Major Professor

TABLE OF CONTENTS

LIST OF FIGURES

LIST OF FIGURES CONTINUES

LIST OF TABLES

ACKNOWLEDGEMENTS

I would like to thank my advisor, Dr. Jin Li for her continual guidance and support throughout this study. I would like to thank Dr. Erik Christensen and Dr. Junhong Chen for serving in my graduate committee. I would further thank Dr. Christensen and the Interim Dean, Dr. Al Ghorbanpoor for their support in obtaining funds for my graduate education.

I am very grateful for the financial support from the University of Wisconsin System Solid Waste Research Program, and technical support provided by WE Energies and the meticulous help given to me in particularly by Bruce Ramme and Dave Kollakowsky. I am indebted to Steve Race and Bob Meidl for their tireless efforts to make the Pilot Scale (Air Slide) apparatus work.

CHAPTER 1: INTRODUCTION

Mercury is a naturally occurring element, which is released into the environment by natural and anthropogenic activities. Natural sources include volcanic activity, weathering of the earth's crust, and bioactivity. According to EPA's 1997 *Mercury study Report to Congress*, coal-fired electric utilities, municipal waste combustors, and medical waste incinerators are the highest emitters of mercury to the air.[1]

US coal-fired power plants emit mercury in three different forms: oxidized mercury (Hg^{2+}, Hg_2^{2+}) (likely to be deposited within the United States); elemental mercury, (Hg^0), which travels many miles before getting deposited on land and in water, and mercury in particulate form, (Hg_p^0).[2] Once deposited in water, mercury is transformed into methyl mercury, a highly toxic form of mercury. Methyl mercury, bioaccumulates in fish and animal tissues, and pose a great health danger to those that eat contaminated fish and other animal tissues. High exposures to mercury have adverse effects on the central nervous system, pulmonary and kidney functions, and causes damages to chromosomes.[3] Human fetus exposed to methyl mercury may be at increased risk of poor performance on neurobehavioral tasks such as those measuring attention, fine motor function, language skills, visual spatial abilities and verbal memory.[2] All types of mercury (both inorganic and organic occurrence in the coal) can be released completely during combustion to the elemental mercury form when the temperature is higher than 650^oC.[4]

Recent estimates of annual total global mercury emissions from natural and human-generated sources range from 4400 to 7500 tons.[2] Human-caused U.S. mercury emissions and U.S. coal-fired power plants are estimated to account for 3% and 1% of global total respectively.[2] Whereas 75 tons annual mercury emission from U.S. coal-fired power plants

may look small as compared to global total, human health concerns associated with mercury exposure warrants mercury emission control.

On March 15, 2005, the US Environmental Protection Agency (EPA) issued the first ever federal rule to permanently cap and reduce mercury emissions from coal-fired power plants. The rule referred to as The Clean Air Mercury Rule (CAMR) when fully implemented, will reduce utility emissions of mercury from 48 tons a year to 15 tons by 2018, a reduction of nearly 70% [2]. The CAMR will compel new coal-fired power plants (construction starting on or after January 30 2004) and existing coal-fired power plants to limit their mercury emissions to 38 tons beginning 2010, and finally cap their emissions to 15 tons beginning 2018[2]. These mandatory caps coupled with significant penalties for noncompliance, will ensure that mercury reduction is achieved and sustained[2].

In anticipation of this rule, scientists and organizations in collaboration with EPA and US Department of Energy (DOE) are carrying out research to understand the science of mercury speciation, and its fate and transport within the atmosphere, in order to develop more efficient and cost-effective mercury control technologies and devices.

The use of activated carbon as a sorbent to remove elemental mercury from coal combustion flue gas is widely accepted as one of the most developed and commercially viable alternative. In this case, activated carbon is injected into the flue gas downstream of a primary particulate collection device, and upstream of a second particulate collection device, commonly referred to as TOXECON^{TM} technology. The activated carbon and mercury mixture is collected separately from the fly ash, thereby preserving the quality of fly ash for use in concrete production. Results from previous bench scale study[5] indicate that there is a potential to liberate elemental mercury, and regenerate and reuse exhausted

activated carbon through thermal desorption, which would significantly reduce the cost associated with the TOXECON^{TM} process. Also, unlike granulated activated carbon (GAC), spent powdered activated carbon (PAC) is usually incinerated, not regenerated for reuse.[65] No document was found to explain why regeneration of PAC has never been done. Without regeneration, the application of PAC for mercury removal can be very costly[65].

The objectives of this study are to demonstrate that mercury adsorbed by activated carbon (TOXECON^{TM} process) can be liberated by thermal methods using a pilot scale apparatus; the Air Slide with and without transition metal oxide catalysts, and captured by a control device (fabric filter).The efficiency of mercury removed from the PAC will be determined by measuring the total mercury left in the PAC after thermal treatments. The bench scale experiments using the Thermogravimetric Analyzer (TGA) will also be performed to demonstrate that elemental mercury can be liberated with a higher efficiency in a controlled environment. The regenerated PAC samples will also be evaluated in terms of change in both mercury concentration and external pore structure by Scanning electron microscopy (SEM), and carbon loss in the PAC measured by loss on ignition (LOI) test.

CHAPTER 2: BACKGROUND AND LITERATURE REVIEW

2.1 The adsorption process

Activated carbon is an amorphous carbon in which a high degree of porosity has been developed during manufacture. This porosity together with high surface area determine the performance of its intended function; adsorption. In general, activated carbon is sometimes described as having a 'crumpled' layered surface, in which flat sheets are broken and curved back upon themselves.[6,7] This unique structure (figure 1) creates activated carbon's very large surface area.[7] The large surface area provides many sites (figure 2)[8] upon which the adsorption of impurity molecules takes place.[9-11] In these sites, pores of different sizes with specific functions exist. The distribution of these pores is the principal factor determining the adsorption characteristics of activated carbon.[12,13]

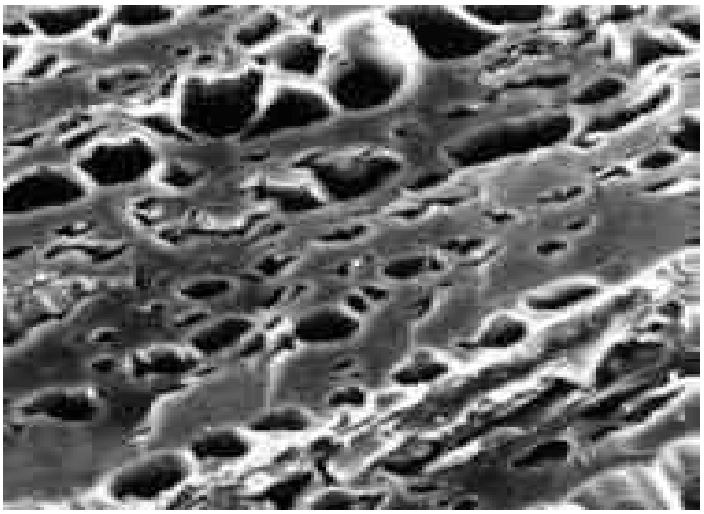

Figure 1: View of pore structure of activated carbon by Scanning Electron Microscope[8]

Once the surface area is covered by the adsorbates, adsorption ceases, and breakthrough occurs. The spent adsorbent must therefore be processed to remove the adsorbate before the carbon can be used again. Moreover, the spent AC itself may be considered a hazardous waste requiring a special treatment facility.[14] Processing involves regeneration of the carbon to restore the pore structure, volume and distribution. According to Sing et al[15] and Bansal et al[16] pores are classified into three categories based on their sizes (figure 2). *Macropores* are cavities of diameter greater than 50nm, used as entrance to the activated carbon by adsorbate molecules. *Mesopores* are pores of diameter between 2 and 50nm, and are used for transportation and adsorption of larger molecules, which cannot gain access to smaller pores. *Micropores* are the smallest category of pores. Their diameter is less than 2nm, and provides activated carbon with most of their surface area and adsorption characteristics (figure 3).[11]

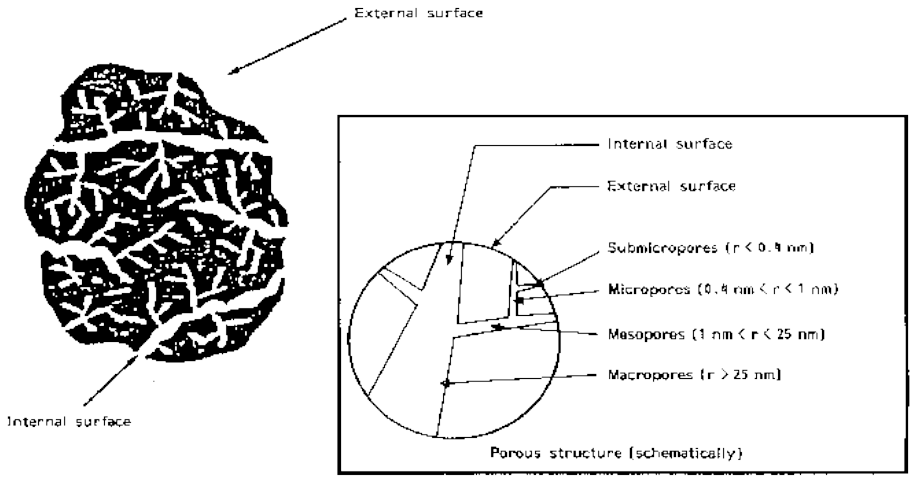

Figure 2: Schematic activated carbon model[11]

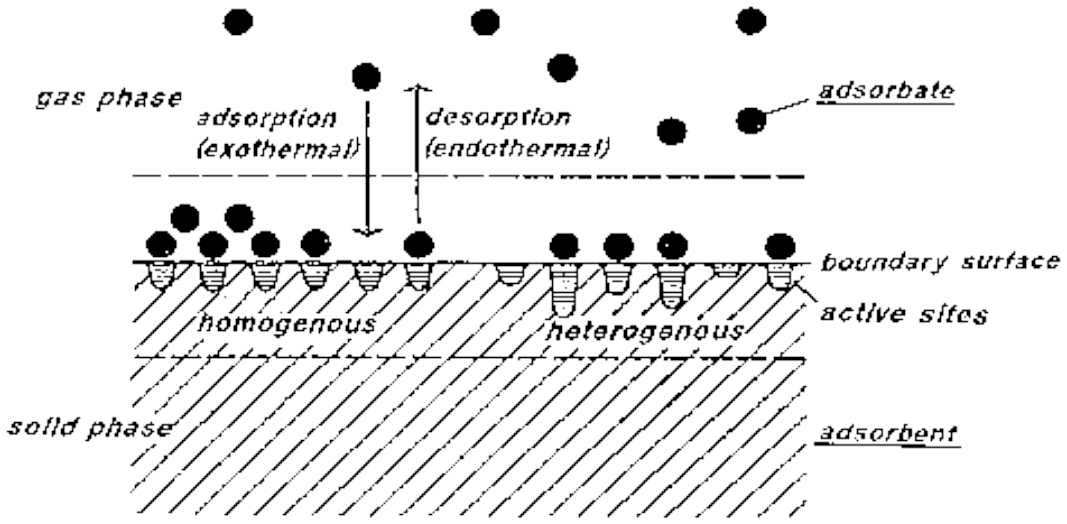

Figure 3: Fundamentals of adsorption and desorption[11]

2.2 Factors affecting adsorption

Adsorption capacity of activated carbon depends on surface area of the activated carbon, adsorption temperature, porosity, pore size distribution, concentration of the adsorbates, type of adsorbate, and the oxygen functional groups in the active centers of the activated carbon.[6,10,13,17-19] Mercury adsorption, in particular, is influenced by many factors including the type of mercury being adsorbed, flue gas composition, adsorption temperature, the inlet mercury concentration, and the gas flow rate.[20,21] Efremenko et al[6], Mundale et al.[22], and Demirbas et al[23] have indicated that the high adsorption capacity of activated carbon is attributed to the surface oxygen functional groups. Studies done by Skodas et al[10] and Li et al[17] have shown that lactone and carbonyl functional groups are the active sites for elemental mercury (Hg^0) adsorption. However, phenol groups and high CO/CO_2 ratio inhibit Hg^0 adsorption. But these oxygen complexes may be removed from

activated carbon surface by heating to 990^{o}C [24]. This is one of the reasons why activated carbon loose adsorption capacity overtime upon regeneration[22].

Li et al[25] performed experiments using bituminous-coal-based activated carbon and activated carbon fiber to determine the role of activated carbon surface moisture in capturing Hg^0 in a bench-scale fixed-bed reactor at room temperature (27^{o}C). The results showed that when both activated carbon samples were heated at 110^{o}C prior to Hg^0 adsorption experiments, about 75-85% reduction in Hg^0 adsorption occurred in both samples despite extreme differences in their ash contents. This result suggested that surface oxygen complexes provide the active sites for mercury bonding. These oxygen complexes are provided by the adsorbed water (H_2O), and the removal of H_2O from the activated carbon surface by low-temperature heat treatment reduces the number of active sites that can chemically bond Hg^0 or eliminates the reactive conditions that favor Hg^0 adsorption.[25]

Carey et al[20] and Olson et al[26] have also shown that the adsorption of elemental mercury on activated carbons is also greatly affected by acidic species such as hydrogen chloride (HCl), sulfur dioxide (SO_2), and nitrogen oxides (NO_x) present in coal combustion flue gases. Sulfur impregnation[27] and halogenated PAC injection[28,29] also improve Hg^o adsorption.

The presence of HCl in the flue gas has been found to enhance Hg^o oxidation. Several researchers have studied this and reported that significant mercury oxidation occur at higher concentration of HCl or Cl_2, at temperatures above 500^{o}C.[3,30-32] Also, Cl_2 was found to be more effective than HCl. Shao et al[33] established that coal chlorine is released primarily as HCl in the high temperature zone of a boiler, but as combustion gases cool,

HCl is partially oxidized to Cl_2 by the Deacon process[1] reaction between O_2 and H_2O. HCl emission depends on temperature and coal type.[34,35] As temperature increases, HCl emission increases proportionately. Likewise, high chlorine coals show greater HCl emissions. The addition of SO_2 to the moist flue gas at high SO_2:HCl ratios decrease the oxidation of Hg^0 [36]. This is attributed to a scavenging effect of SO_2 and H_2O on Cl_2. Richardson et al[37] investigated the addition of halides to the coal or into the boiler. The results shown that high levels of Hg^{2+} occurred in the flue gas when HCl was added to the pilot scale coal combustion unit, but there was no appreciable effect when HCl was added downstream of the combustion boiler. This suggests that the reactions involving chlorine compounds affecting mercury speciation must be initiated in the boiler.

The effect of regeneration temperature and residence time has also been studied. Van Denventer et al[38] have reported that temperature rather than the duration of regeneration influence the adsorptive behavior of activated carbon.

Adsorption can be either physical or chemical. Physisorption is an exothermic process, which occurs because the surface microstructure of activated carbon having high energy due to activation, attract other molecules by weak Van der Waals forces. Chemisorption occurs when the attraction is accomplished by means of a chemical reaction. During adsorption, the micropores, mesopores, and macropores capture both organic and inorganic adsorbates within the porous structure of the activated carbon. These adsorbates must be desorbed and the activated carbon porous structure restored or regenerated with minimal carbon loss.[13,39]

Unlike adsorption, desorption is an endothermic process favored by higher temperature. As temperature increases adsorption decreases but desorption increases. One

[1] Deacon process is used industrially to convert HCl to Cl_2 at temperatures 430-475 ^{o} C with metal catalyst.

of the most widely used methods for regeneration of activated carbon is by thermal means. Thermal regeneration is influenced by type of adsorbate, furnace atmosphere, temperature, and residence time[40]. It involves vaporization of the volatile adsorbates (200-500^{o}C), pyrolysis of the non-volatile adsorbates (500-700^{o}C), and selective oxidation of the pyrolyzed residue (700-850^{o}C).[14, 17, 40-46] Li et al[25] have reported that desorption of the adsorbed mercury occurs at temperatures much higher than the adsorption temperature, suggesting that chemisorption of Hg^0 is the dominant process over physisorption for the moisture-containing activated carbon. Dunham et al[47] have also shown that when adsorbed Hg^0 desorbs from activated carbon, it is in the oxidized form.

San Miguel et al[48] compared GAC regeneration using both thermal (in nitrogen atmosphere) and conventional oxidizing (steam) conditions. The results showed that steam is slightly more effective than nitrogen at regenerating the total micropore volume and BET surface area of the activated carbon. However, greater carbon loss and damage to the pore structure rendered steam regeneration less viable. Activated carbon regeneration in nitrogen atmosphere exhibited greater adsorption capacities for the adsorption of smaller molecular size compounds such as phenol from solution, while activated carbons regenerated in steam adsorbed larger molecular size compounds such as methyl blue more effectively. In general, when product yields were taken into consideration, inert regeneration was found to produce significantly better results than steam regeneration.

2.3 Effects of catalysts on mercury removal and regeneration

The use of transition metal oxide catalysts to enhance decomposition rates at low AC regeneration temperature and residence times have been studied. Dranca et al[53]

established that impregnation of the activated carbons with catalysts facilitates thermal regeneration, and make it occur at lower temperatures between 300-370^{o}C. Coss et al[54] observed that catalytic oxidation can reduce the required temperature by hundreds of degrees, and can save considerable amounts of space for equipment as compared to thermal regeneration. Also, catalytic oxidation performs best when the gas flow rates are nearly constant and at temperatures above 260^{o}C[54]. Sheintuch et al[14] and Matatov-Meytal et al [42, 45] used AC impregnated with CuO, CoO, Cr_2O_3, Fe_2O_3, NiO, and their mixtures to regenerate phenol-exhausted GAC. The results showed that AC impregnated with a mixture of Fe_2O_3 and CuO with small additions of Cr_2O_3 or with carbon pretreatment by inert silica to suppress the carbon ignition, in flowing air restored almost all of its original adsorption capacity even after 10 cycles of regeneration, and the presence of metal oxides in the AC pores did not affect the shape of equilibrium adsorption isotherms. Maria et al[50], used AC impregnated with CoO, Co_3O_4, and CrO_3 catalysts to enhance catalytic oxidation of benzene. The results showed that when impregnation was performed after activation, the impregnated species were deposited on the internal structure, blocking part of the internal porous texture. But when impregnation was performed before activation, the metal species acted as catalysts during the activation step, allowing better catalyst distribution on a more well-developed mesoporous texture, and Co_3O_4 catalyst supported on almond shells worked best. Using synthetic fly ash rich in cuprous chloride (CuCl), Ghorishi et al[36] established that CuCl catalyst is very reactive that it oxidizes elemental mercury even in the absence of HCl in simulated flue gas.

CHAPTER 3: MATERIALS AND METHODS

3.1 Powdered Activated Carbon (PAC)

The PAC used in this study was a lignite-based PAC. The elemental mercury exhausted PAC (TOXECON^{TM}) was obtained from the Prestle Isle Power Plant facility in Michigan. The PAC samples from the TOXECON^{TM} were used as delivered with no further processing done.

3.2 Catalysts

A mixture of 1% Copper (II) oxide, (CuO) powder and 4% Iron (III) oxide, (Fe_2O_3) powder, and Cuprous chloride, (CuCl) powder (Sigma-Aldrich Corp., Milwaukee, WI) with purity of 99.99%, 99% and 97% respectively were used in this experiment. The Iron (III) oxide powder had a nominal size of 5 μm, whereas copper (I) chloride powder and copper (II) oxide powder were of reagent grade. The copper-Iron mixture was chosen after a successful use by Sheintuch et al[14] and Matatov-Meytal et al[42, 45], whereas CuCl had been successfully used by Ghorishi et al.[36]

3.3 Thermal removal of elemental mercury (Hg^0) from spent PAC and regeneration of exhausted PAC

Elemental mercury was liberated and exhausted PAC was regenerated using the pilot scale Air Slide (figure 4) and bench scale Thermogravimetric Analyzer (TGA). The working temperatures were chosen based on researches by Sheintuch et al[14], Li et al[17], and other researchers.[40-46]

3.3.1 Thermogravimetric Analysis

Thermogravimetric Analyzer TGA-500 (Leco Corporation, St. Joseph, MI) was used to liberate mercury. The thermal stability of the PAC samples was measured by percentage weight loss of the samples during heat treatment. The TGA was run in an inert (N_2) atmosphere to prevent ignition of PAC. Nitrogen flowrate was maintained at 100mL. The heating rate was 10^oC/min. to the target temperature, then maintained at the target temperature for 2 hours before the sample was allowed to cool to room temperature in an inert (N_2) atmosphere. The crucibles were partially covered to reduce heat intensity on the samples.

3.3.2 The Pilot Scale (Air Slide) Apparatus

The use of the pilot scale Air Slide (figure 4) in this study was based on its success use in the pilot scale study of mercury liberation and capture from fly ash reported by Li et al, 2005.[5] Figure 5 shows a flow chat for the pilot scale apparatus. The whole system is mainly divided into five components: conical hopper, air slide, baghouse, burner, and collector underneath the air slide. During each experiment run, samples were fed into the air slide through the conical hopper. A rotary feeder controlled the speed at which the sample goes through the system. Inside the air slide, samples were heated by hot air from the burner. The temperature inside the air slide was controlled by adjusting the air flow rate of the burner. A data logger connected to five thermo couples located at the burner, baghouse, air slide inlet, bed and outlet was used to record the temperature readings. After the thermal treatment, part of the sample went to the collector underneath the air slide (product) and the rest of the sample went to the baghouse (by-product). Hot air from the

baghouse passed through the wet scrubber before being emitted into the ambient environment. The operation procedure is in appendix A.

Figure4. The Pilot scale (Air Slide) apparatus for mercury liberation

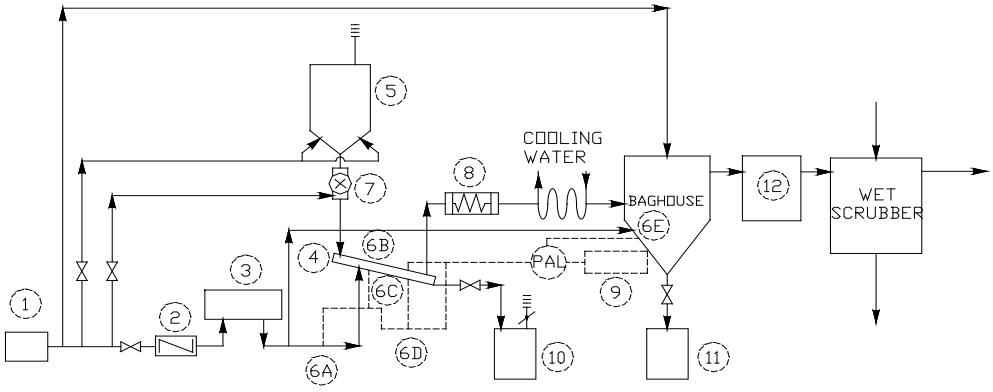

Figure5. Schematic diagram of pilot scale Air Slide

1. Air support 2. Heat exchange 3. 1500 0C furnace 4. Air slide 5. Fly ash feeder 6. Thermal couple 7. Rotary feeder 8. Heat exchange 9. Control panel 10. Ash collection drum 11. Mercury condenser

3.4 Determination of total mercury, moisture content and loss on ignition on spent PAC

The total mercury was determined using the Cold-Vapor Atomic Absorption Method commonly referred to as EPA Method 7471A/245.7. Moisture content and loss on ignition (LOI) were determined in accordance with ASTM Method D5142 and C311 respectively.

3.5 Scanning Electron Microscope (SEM) Analysis on TOXECON samples

3.5.1 Introduction to SEM

The scanning electron microscope (SEM) is a powerful instrument which permits the observation and characterization of heterogeneous organic and inorganic materials such as activated carbon and fly ash samples. The earliest recognized work describing the construction of a scanning electron microscope is that of Von Ardenne in 1938. The first SEM used to examine thick specimens was described by Zworykin et al. (1942)

The scanning electron microscope and electron microprobe are two powerful instruments which permit the observation and characterization of heterogeneous organic and inorganic materials and surfaces. In both instruments, the area to be examined, or the microvolume to be analyzed**,** irradiated with a finely focused electron beam, which may be static or swept in a raster across the surface of the specimen. The types of signals produced when the electron beam impinges on a specimen surface include secondary electrons, and backscattered electrons.

In the SEM, the signals of greatest interest are the secondary and backscattered electrons, since these vary as a result of differences in surface topography as the electron

beam is swept across the specimen. The secondary electron emission is confined to a volume near the beam impact area, permitting images to be obtained at relatively high resolution. The three dimensional appearance of the images is due to the large depth of field of the SEM as well as to the shadow relief of the secondary electron contrast.

The SEM is one of the most versatile instruments available for the examination and analysis of the microstructural characteristics of solid objects. The primary reason for the SEM's usefulness is the high resolution which can be obtained when bulk objects are examined. Values of 5 nm are usually quoted for commercial instruments. Advanced research instruments have reached resolution of about 2.5 nm.

Another important feature of the SEM is the three-dimensional appearance of the specimen image, which is a direct result of the large depth of field. The greater depth of field of the SEM provides much more information about the specimen. In fact, the SEM literature indicates that it is this feature which is of the most value to the SEM user.

The basic components of the SEM are the lens system, electron gun, electron collector, visual and recording cathode ray tubes, and the electronics associated with them. The large depth of field available in the SEM makes it possible to observe three-dimensional objects in stereo. The addition of an energy-dispersive x-ray detector to an electron probe microanalyzer (Fitgerald et al., 1968) signaled the eventual coupling of such instrumentation to the SEM. Today, a majority of SEM facilities are equipped with x-ray analytical capabilities.

To ensure proper construction and record of the SEM image, the following knowledge about the instrument must be considered:

1. The basic scanning action used for the construction of an image;

2. The origin of the commonly encountered contrast mechanisms which arise from the electron-specimen interaction;
3. The characteristics of detectors for the various signals and their influence on the image;
4. Signal quality and its effect on image quality;
5. Signal processing for the final display

Our key concern of this project is whether the thermal treatment in this study will affect the morphology of the PAC particles.

3.5.2 SEM specimen preparation

Particulate samples can usually be examined with little specimen preparation. A thorough discussion of particle collection techniques is given by DeNee (1978). For mounting a number of dry particles at one time, double-stick adhesive tape which has been previously mounted on SEM specimen tabs is used. It should be noted that dry particles tend to agglomerate when handled. The advantage of adhesive tape is that the sticky material has a high enough viscosity so that it does not engulf or climb up over the particles when they are mounted, yet is sticky enough to hold the particles. The particles are transferred to the tape either by a spatula, to deposit a mound of particles or by pouring from a bottle. Loose particles are shaken from the tape since they will produce serious charging effects in the SEM even when they are carbon or metal coated. The tape is often masked with carbon paint to ensure good conductivity to the material in the SEM stub.

Particles can also be attached to SEM stubs by coating the stubs first with aquadag (carbon paint) or a thin layer of parlodian or collodion. The particles are transferred just as the dag or polymer coating has begun to dry. If the particles are mounted too early, they will sink into the “liquid” coating and the surfaces will no longer be useful for SEM examination. If the particles are in a liquid suspension, the particles must be separated from the liquid and placed on an appropriate substrate. If the concentration of particles is relatively high, the particle suspension can be directly put on a substrate by (a) placing a drop or several micro drops onto a substrate with a pipette; (b) spray dispersing the mixture onto a substrate; or (c) filtering the liquid. The liquid is removed by heating, evacuation, solvent exchange, or freeze drying.

The mounting of single particles is more sophisticated, particularly because of the need to keep track of each particle as it is analyzed. Particles greater than 50 μm in size can be mounted directly on normal SEM stubs. They can be selected and placed on the stub by using a stereomicroscope to view the particles during the process. The particles can be handled with stainless tweezers or a fine pointed needle. A vacuum pick can also be used for handling the larger particles. Thin coating of polymer, parlodian, or collodion, can be used to attach the particles to the stub. Also, Aquadag or even Duco cement can be employed. Because of the small area of contact, care must be taken not to distort or crush the particles during mounting. Particles greater than 50 μm in size will become firmly attached when any of these media are in a tacky, partially solidified state. Careful documentation by drawing or optical photos of the particle position and relative size is a necessity.

CHAPTER 4: RESULTS AND DICUSSION

4.1 Mercury removal

4.1.1 The Pilot scale testing using Air Slide

The Pilot Scale Air Slide's rotary feed rate was fixed at 1200 rpm. Figure 6 shows recorded temperature curve during a test with the air slide. A temperature drop was observed on the air slide immediately after the sample was fed into the system. This could be because the sample absorbed the heat in the system as it was heated up.

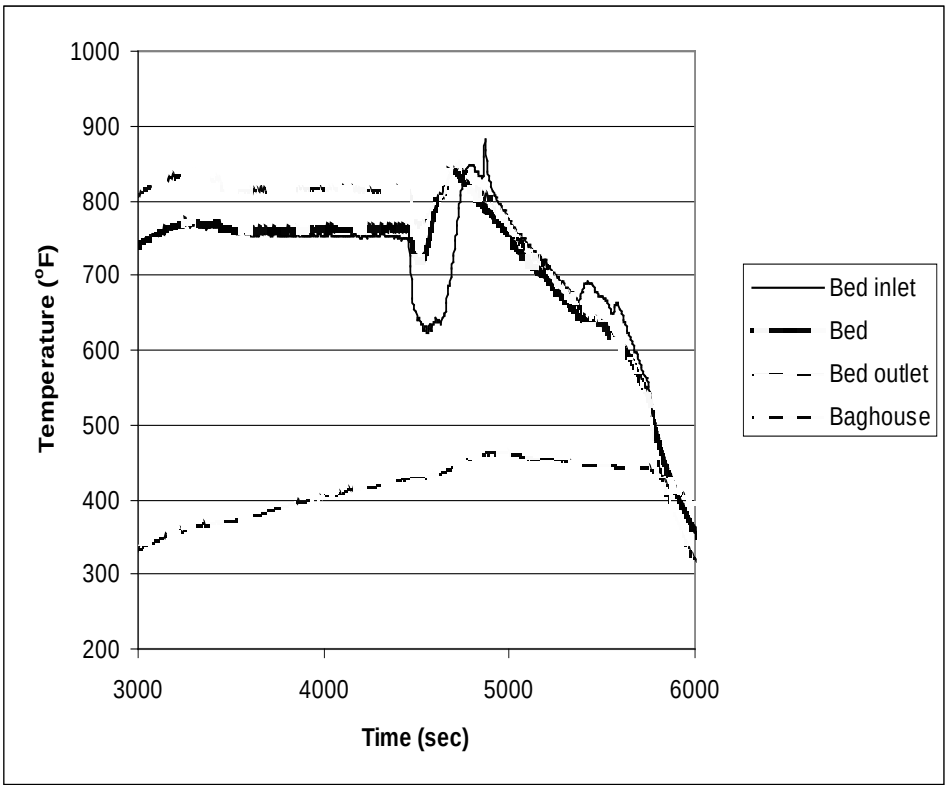

Figure 6: Recorded temperature curve from the air slide at 700^{o}F with catalysts.

A mixture of 1%copper (II) oxide and 4%Iron (III) oxide was used as catalyst in the Air Slide. Table1 shows results of the effect of temperature on mercury removal from the air slide with and without catalysts. The results show that mercury removal increases with temperature without catalysts.

Table1. Effect of temperature on mercury removal using the Air Slide

Test Condition		Without Catalyst		
Rotary Feed Speed (rpm)		1200		
Temperature (^{o}F)		900	1000	1200
Samples as Delivered	Sample Wt. (kg)	1.000	1.066	1.000
	Hg content (ppm)	37	37	46
	LOI	33.6	33.6	44.2
	Moisture content (%)	1.4	1.4	1.9
Samples collected under the air slide (Product)	Sample Wt. (kg)	0.134	0.096	0.026
	Hg content (ppm)	13	6.4	3.7
	%Hg removed	64.9	82.7	92.0
	LOI	27.0	41.2	17.8
	Moisture content (%)	25.4	19.2	9.0
Samples collected in the Baghouse (By-product)	Sample Wt. (kg)	0.280	0.47	0.197
	Hg content (ppm)	69	36	27
	% Change in Hg	86.5	2.7	41.3
	LOI	26.6	35.4	27
	Moisture content (%)	4.9	3.7	7.1

4.1.2 Bench scale tests using the TGA

Bench scale tests were done by the TGA with a retention time of 2 hours in an inert atmosphere without addition of catalysts gave 100% mercury removal beyond 800^{o}F (Table 2). 5%cuprous chloride (CuCl) and a mixture of 1%copper (II) oxide and 4%Iron (III) oxide catalysts were used in the bench scale tests. The results show that 100% mercury removal was achieved by both catalysts from 700^{o}F and above (Table 3). At

800^{o}F without catalysts, mercury removal was 46% in the TGA, but with a mixture of 1%CuO and 4%Fe_2O_3 and 5%CuCl over 97% and 100% mercury removal respectively was achieved at 700^{o}F (Figure 7). This shows that higher mercury removal can be achieved at lower temperatures with catalysts, which confirms an observation earlier made by Sheintuch et al[14], and Matatov-Meytal et al.[42,45]

Table2. Effect of temperature on mercury removal using the Thermogravimetric Analyzer (TGA) (without catalysts)

Temperature (^{o}F)		800	900	1000	1100
Before the test	Hg content (ppm)	54.0	54.0	54.0	54.0
	LOI	44.9	44.9	44.9	44.9
	Moisture content (%)	3.5	3.5	3.5	3.5
After the test	Hg content (ppm)	29.0	0.0	0.0	0.0
	%Hg removed	46.0	100.0	100.0	100.0
	LOI	38.3	35.9	34.4	31.6
	Moisture content (%)	1.8	2.3	1.6	1.6

Table 3: Effect of temperature on mercury removal using the TGA with catalyst (The negative values indicate that mercury increased)

Temperature (^{o}F)		500	700	900
Before the test	Hg content (ppm)	54.0	54.0	54.0
	LOI	44.9	44.9	44.9
	Moisture content (%)	3.5	3.5	3.5
After the test (Tox+1%CuO+ 4%Fe_2O_3)	Hg content (ppm)	58.0	1.4	0.0
	%Hg removed	-7.4	97.4	100
	LOI	40.9	35.9	32.6
	Moisture content (%)	2.5	2.0	1.8
After the test (Tox+5%CuCl)	Hg content (ppm)	64	0.0	0.0
	%Hg removed	-18.5	100	100
	LOI	40.6	35.0	31.7
	Moisture content (%)	0.8	3.8	2.0

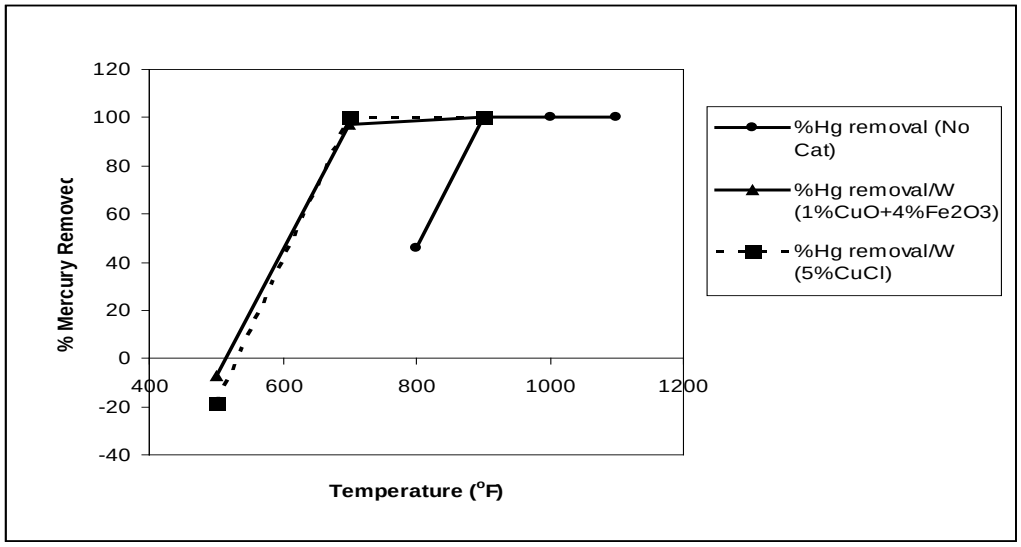

Figure 7. Effect of temperature mercury on removal using the TGA with and without catalysts

4.1.3 Comparison between the pilot scale (Air Slide) and the bench scale (TGA) test.

Mercury removal with the air slide was lower than with the TGA (Tables 1 and 2). For example, at 900^{o}F, 1000^{o}F and 1200^{o}F, the air slide removed only 65%, 83% and 92% of mercury respectively, whereas at the same temperature the TGA had 100% mercury removal (figure 8). In addition, samples collected under the air slide had lower mercury content than those collected in the baghouse. This observation had earlier been made by Li et al[5] during the pilot scale tests with fly ash. Samples collected from the baghouse were also wet as compared with those collected under the air slide. The most probable cause of this could be the baghouse cooling water providing a cooler environment for the vaporized moisture from the PAC and the volatile desorbed mercury got condensed and adsorbed back onto the PAC.

Whereas the gravimetric analysis using the TGA is very accurate and precise, the pilot scale (Air Slide) apparatus is not. Due to this inaccuracy, it was difficult to achieve a mass balance (Table 1). A lot of material was lost probably because accumulation at the Air Slide bed, leakages from the baghouse and/or the Air Slide, and combustion of the PAC. However, the material recovered from the baghouse was more than the product collected under the Air Slide in all the tests performed.

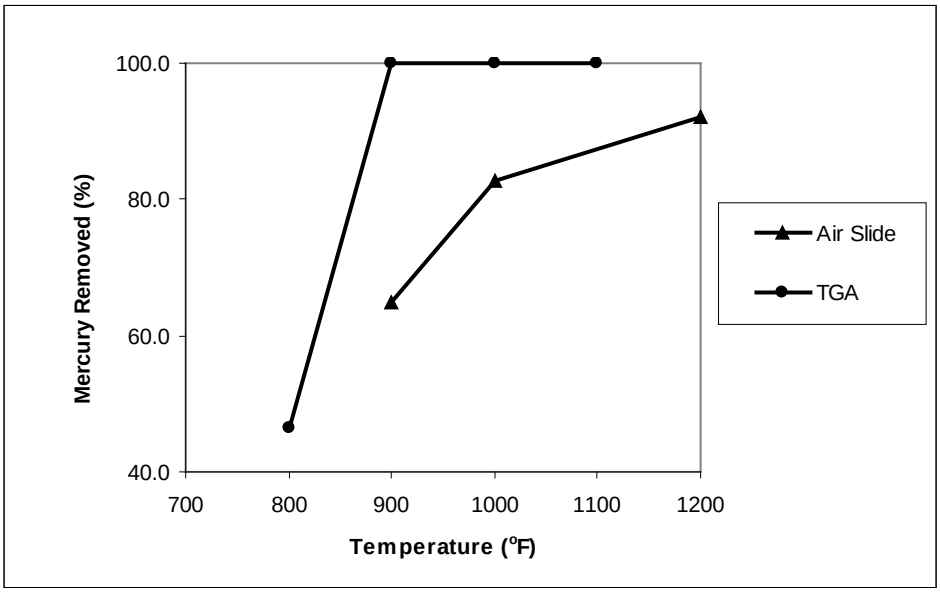

Figure 8. Effect of temperature on mercury removal without catalysts

4.2 Loss on ignition (LOI)

Loss on ignition (LOI) is used as an indicator of carbon content in the PAC because carbon is the main contributor to the LOI. However, carbon content and LOI are different. LOI is simply the difference in weight after the sample is heated up to 750^{o}C for several hours.

4.2.1 The pilot scale Air Slide

There was no trend in the variation of temperature with LOI for samples tested with the Air Slide (Table 1). For example, at 900^{o}F and 1200^{o}F without catalyst and 600^{o}F with catalyst, there was decrease in LOI, but LOI increased by about 23% and 5% at 1000oF for samples collected in the baghouse and the Air Slide bed respectively (Table 1).

4.2.2 Bench Scale tests using the TGA

The influence of temperature on LOI for samples with and without catalysts tested by the TGA is presented in Figure 9. The results show that LOI decreases with increase in temperature, indicating that PAC carbon loss increases with increase in temperature (figure 10). There is a sharp decrease in LOI for catalyst-treated PAC as compared with PAC without catalysts. This could be attributed to rapid oxidation of the residual material at the active sites of the PAC enhanced by the catalysts. Overall, carbon content, determined by loss on ignition (LOI) reduced by 13%. However, this carbon loss is not expected to have a significant effect on the surface area of the PAC.

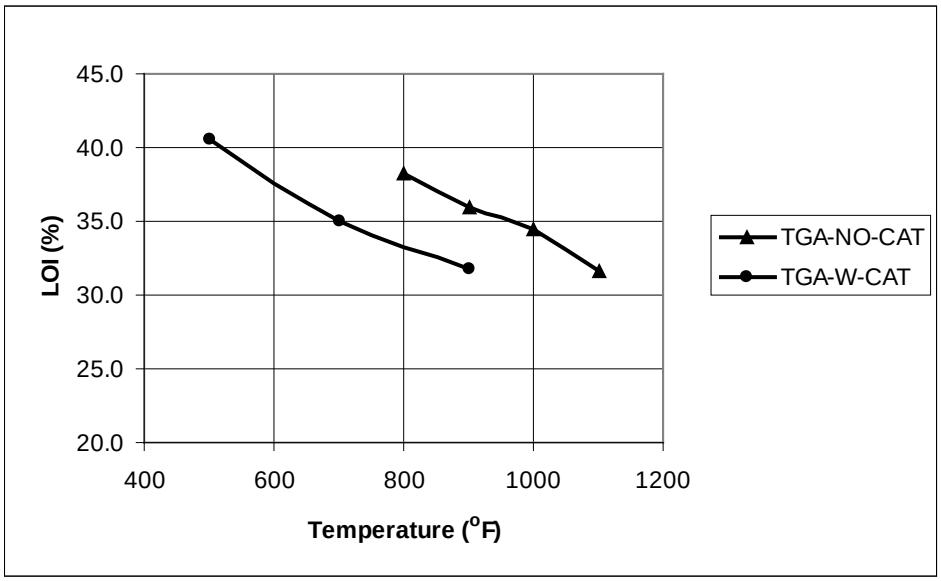

Figure 9: Effect of temperature on LOI for TGA tested PAC with and without catalysts

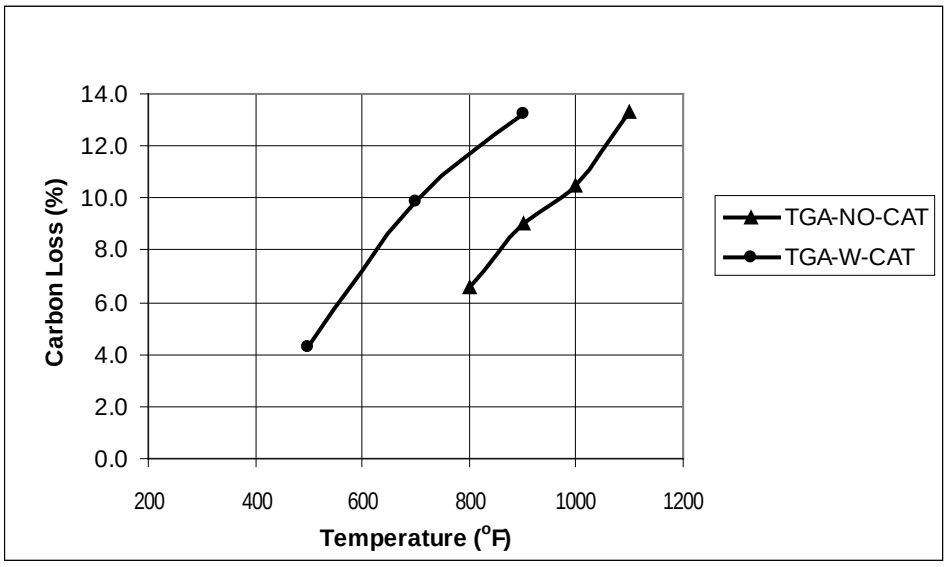

Figure 10. Variation of Carbon loss with temperature for TGA-tested PAC with and without catalysts.

4.3 SEM image analysis

Many SEM (ABT-32, Topcon America Corporation, Paramus, NJ) images were taken at different positions on the sample to study the morphology of the samples before

and after thermal treatment. All SEM images (figure 11 to figure 22) indicated that PAC is composed of fine and coarse particles. The white round particles are mainly fly ash spheres of inorganic compounds. The relatively dark particles are mostly composed of unburned PAC. The black represents the spaces between the particles.

A close comparison of SEM images from TGA test at 700^{o}F with (figure 16) and without (figure 13) catalyst with as delivered PAC samples (figure 11) indicate fine aggregation and some carbon loss on the sample treated with catalyst (figure 16). No change in particle aggregation was observed in the sample without catalyst (figure 13). However, a sample tested at 800^{o}F in the TGA (figure 20) shows some carbon loss. The images from the pilot scale Air Slide were also compared with the as delivered PAC sample image. The by-product (baghouse) sample image (tested at 1200^{o}F) without catalyst (figure 17) show fine aggregation in a cloudy surface indicating some carbon loss. There was no change in aggregation on the product (bed) image (figure 16) as compared with the as delivered sample image (figure 11). SEM images of samples tested at 700^{o}F both at the Bench Scale (TGA) and the Pilot Scale (Air Slide) with and without catalyst treatment were compared. The by-product sample image (figure 19) shows fine aggregation and carbon loss. The TGA images (figures 12 and 13) and the product sample image (figure 18) did not show either change in aggregation or significant carbon loss. Two PAC samples treated with a mixture of 1%CuO and 4%Fe_2O_3 (figure 14) catalyst and another treated with 5%CuCl (figure 15) catalyst, and tested at 900^{o}F were also compared. The former show some carbon loss with no particle aggregation, whereas the latter did not show either particle aggregation or carbon loss.

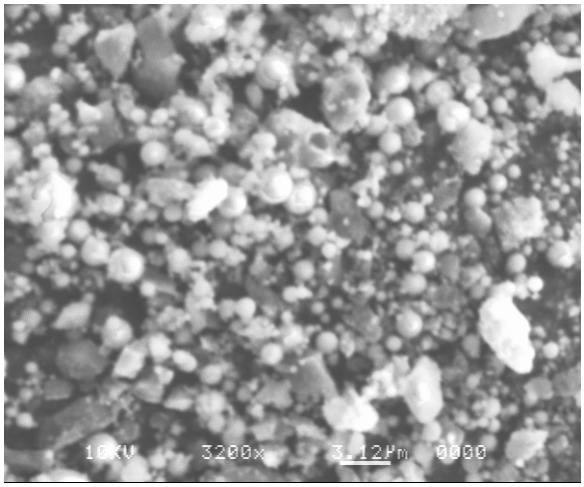

Figure 11: SEM image of PAC sample from the TOXECON process as delivered (X3200)

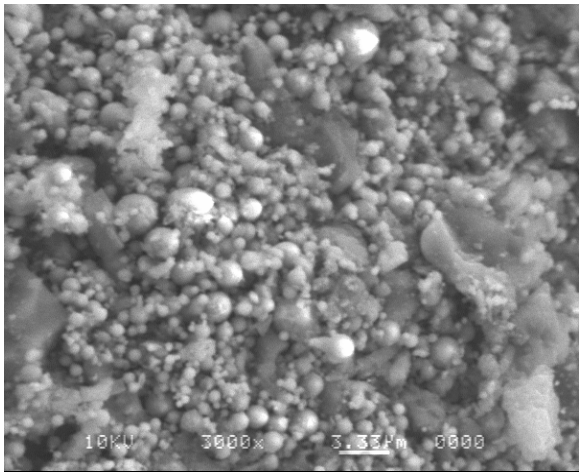

Figure 12: SEM image of PAC sample process at 700^{o}F in the TGA (X3000)

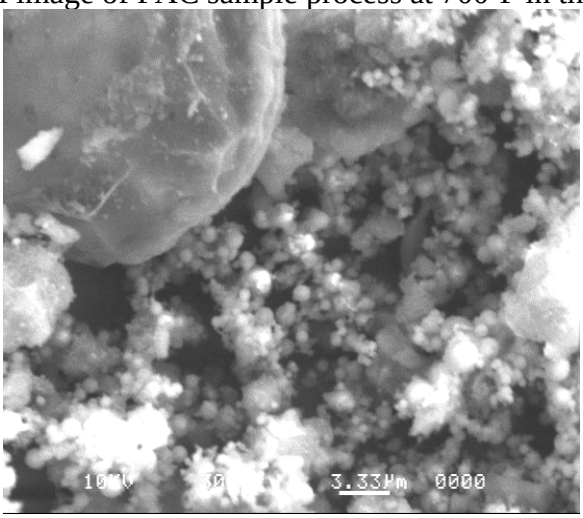

Figure 13: SEM image of PAC sample after addition of a mixture of 1%CuO+4%Fe_2O_3 catalyst at 700^{o}F with in an inert atmosphere in the TGA (X3000)

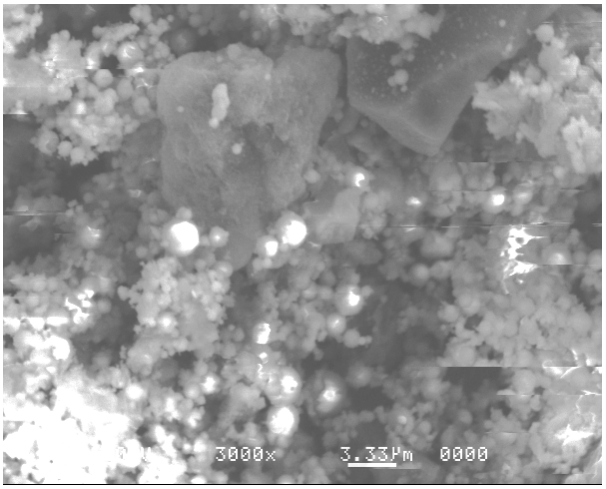

Figure 14: SEM image of PAC sample after addition of a mixture of %CuO+4%Fe_2O_3 catalyst and heated at 900^{o}F in an inert atmosphere in the TGA (X3000)

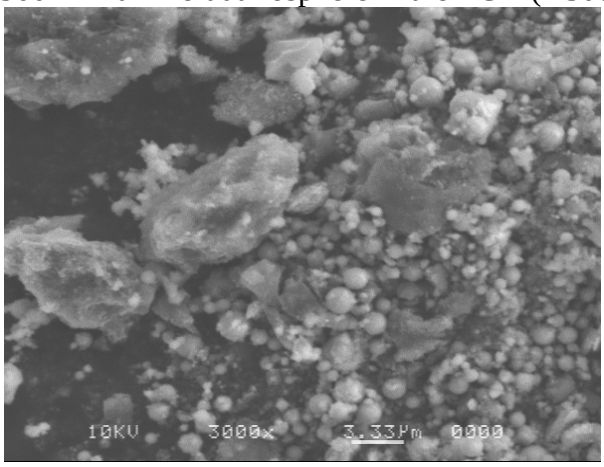

Figure 15: SEM image of PAC sample from the TOXECON^{TM} process after addition of 5%CuCl catalyst and heated at 900^{o}F for 2 hrs in an inert atmosphere in the TGA (X3000)

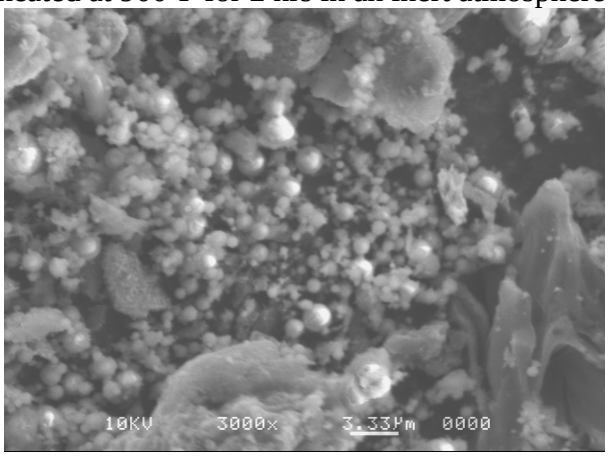

Figure 16: SEM image of PAC sample from the TOXECON^{TM} process after thermal treatment at 1200^{o}F for 3-4 min without catalyst in the air slide bed (X3000)

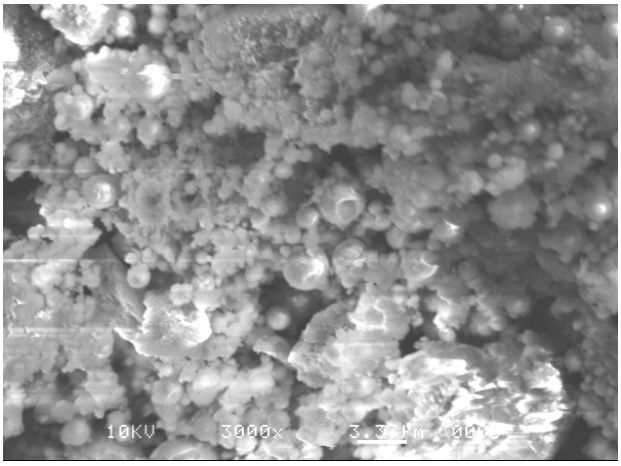

Figure 17: SEM image of PAC sample from the TOXECON^{TM} process after thermal treatment at 1200^{o}F for 3-4 min without catalyst in the air slide (baghouse) (X3000)

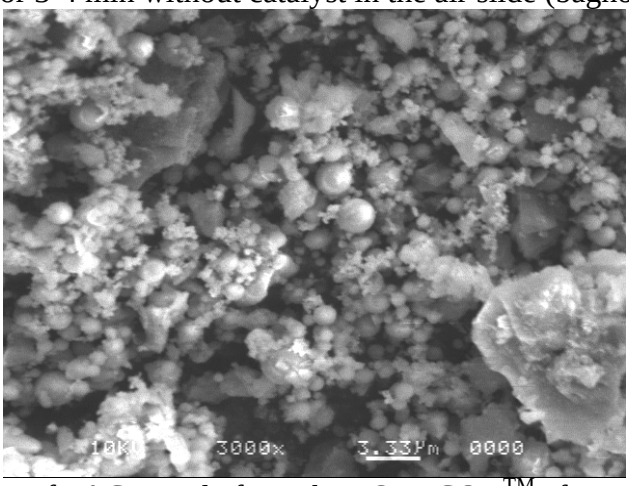

Figure 18: SEM image of PAC sample from the TOXECON^{TM} after addition of a mixture of 1%CuO+4%Fe_2O_3 catalyst and heated at 700^{o}F for 3-4min in the air slide bed (X3000)

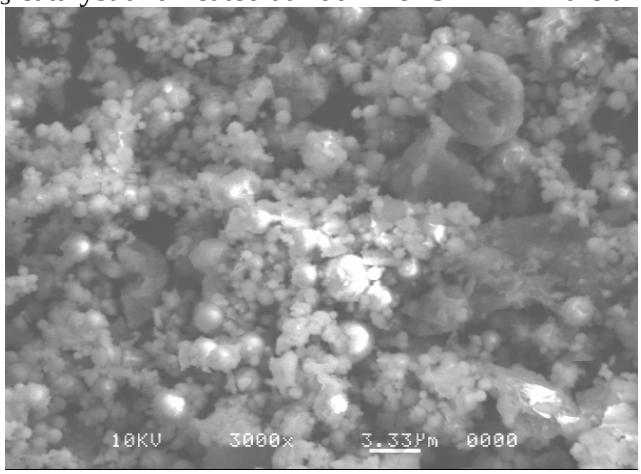

Figure 19: SEM image of PAC sample from the TOXECON^{TM} after addition of a mixture of 1%CuO+4%Fe_2O_3 catalyst and heated at 700^{o}F 3-4min in the Air Slide (baghouse) (X3000)

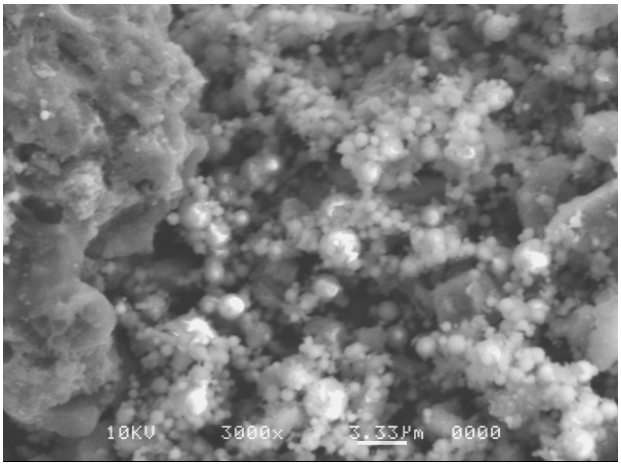

Figure 20. SEM image of PAC sample from the TOXECON process after thermal treatment at 800^{o}F for 2 hrs in an inert atmosphere in the TGA (X3000)

Energy Dispersive X-ray (EDX) analysis was done on the PAC samples before and after thermal treatment to determine changes if any on chemical composition of the particles. The analysis was done on the coarse particles and a selected average area. Results of EDX analysis (figure 20 to 23 and appendix B) showed that the coarse particles have high carbon and are composed of calcium and sulfur (figures 21 and 23); whereas the fine particles were fly ash particles with high aluminum, silicon and magnesium (appendix B). It is believed that calcium and sulfur might have been adsorbed on the carbon surface. There was no dramatic change in particle aggregation in all the tests although by-product (from the baghouse) samples (appendix B) looked finer than the rest. EDX analysis on a coarse particle from the baghouse (appendix B) show less carbon content as compared with the rest of the coarse particles from the bench scale (TGA) test and the air slide bed. This carbon loss and change in aggregation might be attributed to partial combustion of the PAC in the baghouse. All the PAC samples showed high calcium content possibly from the adsorbed mercury; a typical characteristic of western coals from which PAC was made.

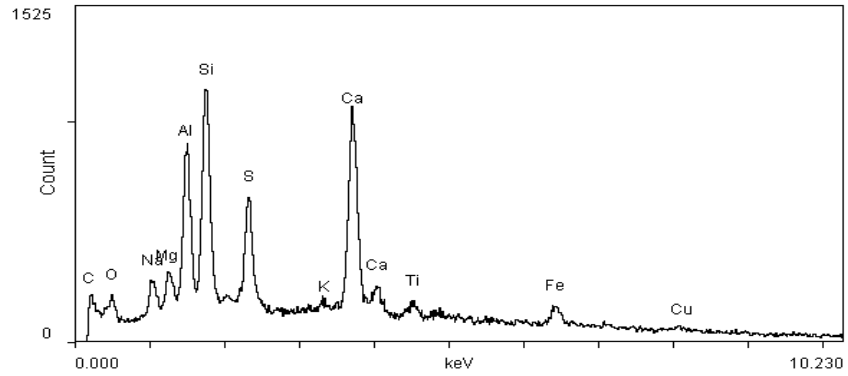

Figure 21: Energy Dispersive X-ray analysis of an average PAC sample area from the TOXECON^{TM} process after thermal treatment for 2 hrs at 1000^{o}F in the TGA (X500)

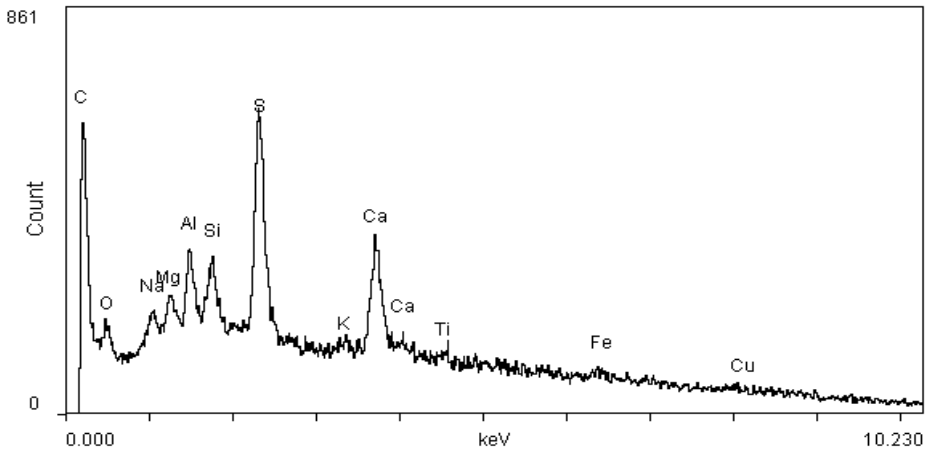

Figure 22: Energy Dispersive X-ray analysis of a coarse PAC particle from the TOXECON^{TM} process after thermal treatment at 1000^{o}F in the TGA (X500)

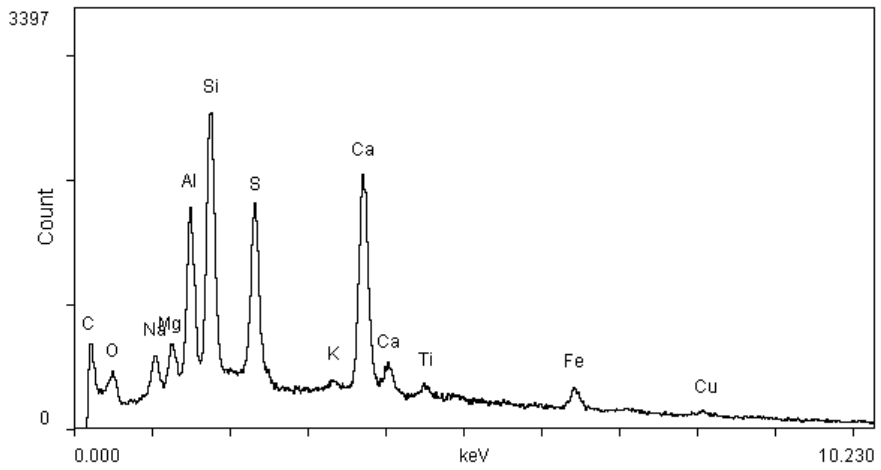

Figure 23: Energy Dispersive X-ray analysis of an average PAC sample area from the TOXECON^{TM} process with a mixture of 1%CuO and 4%Fe_2O_3 catalyst after thermal treatment for 3-4 min at 700^{o}F in the air slide bed (X500)

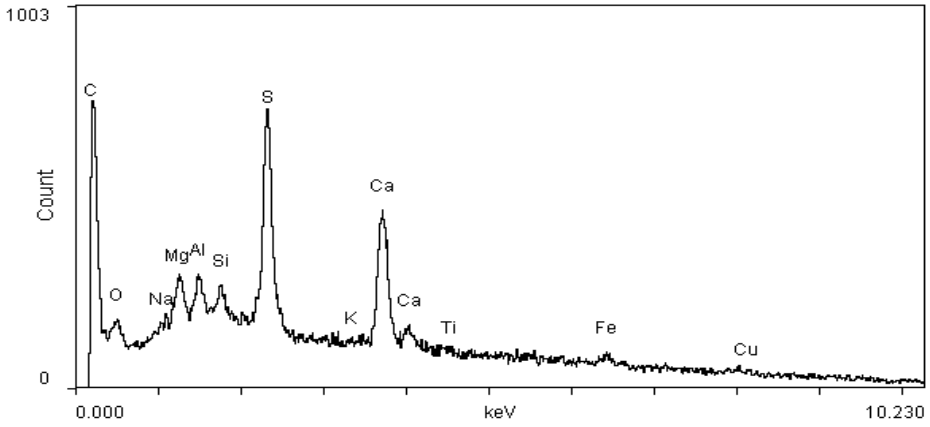

Figure 24: Energy Dispersive X-ray analysis of a coarse PAC particle from the TOXECON^{TM} process after addition of a mixture of 1% CuO+4%Fe_2O_3 catalyst and heated at 700^{o}F for 3-4 min in the air slide bed (X500)

CHAPTER 5: CONCLUSIONS AND RECOMMENDATIONS

5.1 Conclusions

The experimental results have indicated that elemental mercury can be removed by the pilot scale (air slide) apparatus with reasonable efficiency. The bench scale experiment using thermogravimetric analyzer (TGA) removed 29%, 100%, 100%, and 100% at operation temperatures of 800^{o}F, 900^{o}F, 1000^{o}F, and 1100^{o}F respectively without catalysts, and 100% mercury removal with catalysts at 700^{o}F and beyond. This bench scale result demonstrates that mercury can be liberated with a higher efficiency in a controlled environment. It also demonstrates that a mixture of 1% copper (II) oxide (CuO) and 4% Iron (III) oxide (Fe_2O_3) catalyst and 5% cuprous chloride (CuCl) can enhance mercury liberation at lower temperatures. The catalytic performance of 5% cuprous chloride (CuCl) was identical to that of the copper-iron mixture. Carbon loss as determined by LOI was minimal, but increased with temperature to a maximum of about 13% with and without catalysts. SEM analysis on the PAC samples from the TOXECON^{TM} process observed no change in particle aggregation. However, particles from the baghouse looked finer than the rest. In general, thermal treatment had no effect on particle morphology. Energy Dispersive X-ray analysis show that the PAC samples from the TOXECON^{TM} process are composed of coarse and fine particles. The coarse particles were rich in calcium and sulfur embedded in a matrix of carbon; whereas the fines were fly ash particles rich in aluminum, silicon and magnesium. The chemistry of the PAC samples were the same in all the samples examined. Moreover, the adsorption capacity of the regenerated PAC is not expected to be substantially affected by thermal treatment because there was only 13% carbon loss with little or no aggregation of the particles.

5.2 Recommendations

- The Brunauer Emmett and Teller (BET) test need to be performed on the samples to determine the surface area and pore size distribution.
- The adsorption capacity need to assess to determined the hypothesized regeneration.
- The design of the air slide needs to be refined to
    - reduce accumulation of the PAC on the air slide bed
    - assure that the micropores on the air slide bed are open, and enough air goes through them.

REFERENCES

1. Mercury Study to Congress; EPA-452-R-97-003-009; U.S. Environmental Protection Agency (EPA), Washington D.C., 1997.

2. EPA, Clean Air Mercury Rule (CAMR), 2005: Available at http://www.epa.gov/air/mercuryrule (Accessed: July 19, 2006).

3. Pavlish, J.H., Sondreal, E.A., Mann, M.D., Olson, E.S., Galbreath, K.C., Laudal, D.L., Benson, S.A., 2003: "Status Review of Mercury Control Options for Coal-Fired Power Plants," *Fuel Processing Technology 82: 89-165*

4. Liu, K., Gao, Y., Kellie, S., Pan, W-P., Riley, J.T., Ho, K.K., Mehta, A.K., 2001: "A study of Mercury Removal in FBC Systems Fired with High Chlorine Coals," *Combustion Science and Technology, 164: 145-162.*

5. Li, J., Gao,X., Goeckner, B., Kollakowsky, D., Ramme, B., 2005, "A Pilot study of mercury liberation and capture from coal-fired power plant fly ash," *Journal of Air and Waste management Association, 55: 258-264.*

6. Efremenko, I., Sheintuch, M., "Predicting Solute Adsorption on Activated Carbon: Phenol" 2006: *Langmuir: 22(8): 3614-3621.*

7. Pope, J.P., "Activated Carbon and Some Applications for the Remediation of Soil and Groundwater Pollution": 1996.

8. CPL Carbon Link, "Properties of Activated Carbon", www.activated-carbon.com/carbon.html. (Accessed on May 19, 2006).

9. Martin, R.J., Ng, W.J., "The Repeated Exhaustion and Chemical Regeneration of Activated Carbon" 1987: *Wat. Res. 21(8): 961-965.*

10. Skodras, G., Diamantopoulou, Ir., Natas, P., Palladas, A., Sakellaropoulos, G.P., "Postcombustion Measures for Cleaner Solid Fuels Combustion: Activated Carbons for Toxic Pollutants Removal from Flue Gases" 2005: *Energy & Fuels: 19(6): 2317-2327.*

11. Henning, K.-D., Schafer, S., "Impregnated activated carbon for environmental protection" *Paper presented at the meeting of the European Rotogravure Association Engineers Group, Mulhouse, France, March 20-21, 1990.*

12. Chiang, Y-C., Chiang, P-C., Huang, C-P., "Effects of pore structure and temperature on VOC adsorption on activated carbon" 2001: *Carbon: 39: 523-534.*

13. Miguel, G.S., Lambert, S.D., Graham, N.J.D., “The regeneration of field-spent Granular Activated Carbons” 2001: *Wat. Res. : 35(11): 2740-2748.*

14. Sheintuch, M., Matatov-Meytal, Y.I., 1999: “Comparison of catalytic processes with other regeneration methods of activated carbon” *Catalysis Today, 53: 73-80.*

15. Sing, K.S.W., Everett, D.H., Haul, R.A.W., Moscou, L., Pierotti, R.A., Rouquerol, J., Siemieniewska, T., 1985: “Reporting physisorption Data For Gas/Solid Systems: With Special Reference to the Determination of Surface Area and porosity,” *Pure and Applied Chemistry, 57(4): 603-619.*

16. Bansal, R.C., Donnet, J.B., Stoeckli, F., 1988: “Active Carbon,” *New York: Dekker*

17. Li, Y.H., Lee, C.W., Gullett, B.K., “Importance of activated carbon’s oxygen surface functional groups on elemental mercury adsorption” 2003: *Fuel: 82: 451-457.*

18. Ania, C.O., Parra, J.B., Pevida, C., Arenillas, A., Rubiera, F., Pis, J.J., “Pyrolysis of activated carbons exhausted with organic compounds” 2005: *J. Anal. Appl. Pyrolysis: 74: 518-524.*

19. Brennan, J.K., Thomson, K.T., Gubbins, K.E., “Adsorption of Water in Activated Carbons: Effects of Pore Blocking and Connectivity”2002: *Langmuir: 18(14): 5438-5447.*

20. Carey, T.R., Hargrove, Jr., O.W., Richardson, C.F., “Factors Affecting Mercury Control in Utility Flue Gas Using Activated Carbon” 1998: *Journal of the Air & Waste Management Association: 48:1166-1174.*

21. Ho, T.C., Kobayashi, N., Lee, Y., Lin, J., Hopper, J.R., 2004: “Experimental and Kinetic Study of Mercury Adsorption on Various Activated Carbons in a Fixed-Bed Adsorber” *Environmental Engineering Science, 21(1): 21-27.*

22. Mundale, V.D., Joglekar, H.S., Kalam, A., Joshi, J.B., “Regeneration of Spent Activated Carbon by Wet Air Oxidation” 1991: *The Canadian Journal of Chemical Engineering: 69: 1149-1159.*

23. Demirbas, A., Arslan, G., Pehlivan, E., 2006: “Recent Studies on Activated Carbons and Fly Ashes from Turkish Resources” *Energy Sources, Part A., 28(7): 627-638.*

24. Walker, JR., P.L., Taylor, R.L., Ranish, J.M., “An update on the Carbon-Oxygen Reaction” 1991: *Carbon: 29(3): 411-421.*

25. Li, Y.H., Lee, C.W., Gullet, B.K., 2002: "The effect of activated carbon surface moisture on low temperature mercury adsorption" *Carbon, 40: 65-72.*

26. Olson, E.S., Laumb, J.D., Benson, S.A., Dunham, G.E., Sharma, R.K., Miller, S.J., Pavlish, J.H., 2003: "The Multiple Site Model for Flue Gas-Mercury Interactions on Activated Carbons: The Basic Site" *Fuel Chemistry Division Preprints, 48(1): 30-31.*

27. His, H.-C., Rood, M.J., Rostam-Abadi, M, Chen, S., Chang, R., "Mercury Adsorption Properties of Sulfur-Impregnated Adsorbents" 2002: *Journal of Environmental Engineering: 128(11): 1080-1089.*

28. U.S. Environmental Protection Agency: Air Pollution Prevention and Control Division, "Control of Mercury Emissions from Coal Fired Electric Utility Boilers: An Update, February 18, 2005.

29. EPRI: Status of Mercury Control Technologies: Activated Carbon Injection and Boiler Chemical Additives: *Final Technical Report, March 2006.*

30. Widmer, N.C., Cole, J.A., Seeker, W.R., Gaspar, J.A., 1998: "Practical Limitation of Mercury Speciation in Simulated Municipal Waste Incinerator Flue Gas" *Combust. Sci. and Tech., 134: 315-326.*

31. Widmer, N.C., West, J., Cole, J.A., 2000: "Thermochemical Study of Mercury Oxidation in Utility Boiler Flue Gases" *In: Proceedings of the Air & Waste management Association's 93rd Annual Meeting & Exhibition, Salt Lake City, Utah, June 18-20, 2000.*

32. Kellie, S., Cao, Y., Duan, Y., Li, L., Chu, P., Mehta, A., Carty, R., Riley, J.T., Pan, W., 2005: "Factors Affecting Mercury Speciation in a 100-MW Coal-Fired Boiler with Low-NOx Burners," *Energy and Fuels, 19: 800-806.*

33. Shao, D., Hutchinson, E.J., Cao, H., Pan, W-P., Chou, C-L., 1994: "Behavior of Chlorine during Coal Pyrolysis" *Energy & Fuels, 8(2): 399-401.*

34. Xie, W., Pan, W.-P., Riley, J.T., "Behavior of chloride during coal combustion in an AFBC System, "*Energy and Fuels; 1999, 13, pp 585-591.*

35. Kilgroe, J., Senior, C., "Fundamental Science and Engineering of Mercury Control in coal-fired power plants," *In proceedings of the Air Quality IV Conference, Sept. 22-24, 2003, Arlington, VA.*

36. Ghorishi, B.S., Lee, C.W., Jozewicz, W.S., Kilgroe, J.D., 2005: "Effect of Fly Ash Transition Metal Content and Flue Gas HCl/SO_2 Ratio on Mercury Speciation in Waste Combustion," *Environmental Engineering Science, 22(2): 221-231.*

37. Richardson, C., Machalek, T., Marsh, B., Miller, S., Richardson, M., Chang, R., Strohfus, M., Smokey, S., Hagley, T., Juip, G., Rosvold, R., 2003: "Chemical Addition for Mercury Control in Flue Gas Derived from Western Coals, Paper #63.

38. Van Deventer, J.S.J., Camby, B.S., 1988: "The Influence of Regeneration Conditions on the Adsorptive Behaviour of Activated Carbon" *Minerals Engineering, 1(2): 157-163.*

39. Mclaughlin, H.S., "Regenerate Activated Carbon Using Organic Solvents" *Chemical Engineering Progress, July 1995.*

40. Avraamides, J., "Thermal regeneration of activated carbons-effect of temperature, time and steam addition on carbon activity" 1987: *Transactions of the Institution of Mining and Metallurgy Section C-Mineral Processing and Extractive Metallurgy: 96: C137-C143.*

41. Bagreev, A., Rahman, H., Bandosz, T.J., 2002: "Sudy of regeneration of activated carbons used as H_2S adsorbents in water treatment plants," *Advances in Environmental Research, 6: 303-311.*

42. Matatov-Meytal, Y.I., Sheintuchi, M., Shter, G.E., Grader, G.S., "Optimal Temperatures for Catalytic Regeneration of Activated Carbon" 1997: *Carbon: 35(10-11): 1527-1531.*

43. Ferro-Garcia, M.A., Utrera-Hidalgo, E., Rivera-Utrilla, J., Moreno-Castilla, C., Joly, J.P., "Regeneration of Activated Carbons Exhausted with Chlorophenols" 1993: *Carbon: 31(6): 857-863.*

44. Van Vliet, B.M., "The regeneration of activated carbon" 1991: *J. S. Afr. Inst. Min. Metall. 91(5): 159-167.*

45. Matatov-Meytal, Y.I., Sheintuch, M., 1997: "Abatement of Pollutants by Adsorption and Oxidative Catalytic Regeneration" *Ind. Eng. Chem. Res., 36(10): 4374-4380.*

46. Manocha, S.M., 2003: "Porous Carbons," *Sadhana, 28, part 1 &2: 335-348.*

47. Dunham, G.E., Miller, S.J., Chang, R., Bergman, P., 1998: "Mercury Capture by an Activated Carbon in a Fixed-Bed Bench-Scale System" *Environmental Progress, 17(3): 203-208.*

48. San Miguel, G., Lambert, S.D., Graham, J.D., 2002: "Thermal Regeneration of Granulated Activated Carbon Using Inert Atmospheric Conditions" *Environmental Technology, 23(12): 1337-1346.*

49. San Miguel, G., Lambert, S.D., Graham, N.J.D., 2003: "The effect of thermal treatment on the reactivity of field-spent activated carbons" *Applied Catalysis B: Environmental, 40: 163-184.*

50. Maria, C.M., Alvim-Ferraz, Carla, M.T.B. Gaspar, 2005: "Impregnated Active Carbons to Control Atmospheric Emissions: Influence of Impregnation Methodology and Raw Material on the Catalytic Activity" *Environ. Sci. Technol., 39(16): 6231-6236.*

51. Jones, D.A., Lelyveld, T.P., Mavrofidis, S.D., Kingman, S.W., Miles, N.J., 2002: "Microwave heating applications in environmental engineering – a review" *Resources, Conservation and Recycling; 34(2)75-90.*

52. Chiang, P.C., Wu, J.S., 1989, "Evaluation of Chemical and Thermal Regeneration of Activated Carbon," *Wat. Sci. Tech., 21: 1697-1700.*

53. Dranca, I., Lupascu, T., Vogelsang, K., Monahova, L., "Utilization of thermal analysis to establish the optimal conditions for regeneration of activated carbons" 2001: *Journal of Thermal Analysis and Calorimetry; 64, 945-953.*

54. Coss, P.M., Chang, Y.C., "Microwave Regeneration of activated carbon used for removal of solvents from vented air: 2000: *Journal of the Air & Waste Management Association, 50:529-535.*

55. Tomasko, D.L., Hay, K.J., Leman, G.W., Eckert C.A., "Pilot Scale Study and Design of a Granular Activated Carbon Regeneration Process Using Supercritical Fluids" 1993: *Environmental Progress: 12(3): 208-217.*

56. Wedeking, C.A., Snoeyink, V.L., Larson, R.A., Ding, J., "Wet Air Regeneration of PAC: Comparison of Carbons with Different Surface Oxygen Characteristics" 1987: *Wat. Res. 21(8): 929-937.*

57. Ho, T.C., Lee, Y., Chu, H.W., Lin, C.J., Hopper, J.R., "Modelling of mercury desorption from activated carbon at elevated temperatures under fluidized/fixed bed operations" 2005: *Powder Technology: 151: 54-60.*

58. Salvador, F., Sanchez Jimenez, C., "Effect of regeneration treatment with liquid water at high pressure and temperature on the characteristics of three commercial activated carbons" 1999: *Carbon: 37: 577-583*

59. Saha, B., Tai, M.H., Streat, M., 2001: "Study of Activated Carbon After Oxidation and Subsequent Treatment: Characterization" *Trans IChemE, Part B., 79(B4): 211-217.*

60. Hashimoto, K., Miura, K., Yoshikawa, F., Imai, I., 1979: “Change in Pore Structure of Carbonaceous Materials during Activation and Adsorption Performance of Activated Carbon” *Ind. Eng. Chem. Process Des. Dev., 18(1): 72-80.*

61. Sabio, E., Gonzalez, E., Gonzalez, J.F., Gonzalez-Garcia, C.M., Ramiro, A., Ganan, J., 2004: “Thermal regeneration of activated carbon saturated with *p*-nitrophenol” *Carbon, 42: 2285-2293.*

62. Aubin, D.G., Abbatt, J.P., 2006: “Laboratory Measurements of Thermodynamics of Adsorption of Small Aromatic Gases to *n*-Hexane Soot Surfaces” *Environ. Sci. Technol., 40(1): 179-187.*

63. Baldassarre, G., Amicarelli, V., 1985: “Low Temperature Regeneration of Activated Carbon II. Kinetic evaluation of consecutive o-NO_2-phenol thermodesorptions” *Journal of Thermal Analysis, 30: 339-343.*

64. Gurses, A., Dogar, C., Acikyildiz, M., Ozkan, E., Bayrak, R., 2005: “Effect of Temperature for the Adsorption of Methylene Blue onto Activated Carbon Produced from Waste Dogrose Seeds” *Acta horticulturae, 690: 277-284.*

65. Fang, C.S., Lai, P.M.C., 1996: “Microwave Regeneration of Spent Powder Activated Carbon” *Chem. Eng. Comm., 147: 17-27.*

66. Ghorishi, S.B., Keeney, R.M., Serre, S.D., Gullett, B.K., Jozewicz, W.S., 2002: “Development of a CI-Impregnated Activated Carbon for Entrained-Flow Capture of Elemental Mercury” *Environ. Sci. Technol., 36(20): 4454-4459.*

APPENDIX A

The PILOT SCALE (AIR SLIDE) APPARATUS

Set-Up Procedures

1. Equipment is placed on a firm, hard surface and components are connected properly and securely. Keep equipment away from flammable items.
2. All switches and controls are set in the off position and valves are closed. Remove the baggie from the gas line connection. Connect external power, air, and gas lines to operating system. Check that connections are secure and there are no leaks. Ensure that the hose connected to the cooling water outlet is in the drain.

Start-up Procedures:

3. The pressure reducing stations for the burner unit should not be adjusted. The automated burner unit is preset and will adjust itself. Changing the air pressure setting may cause the burner to fail at startup. Turn on air lines to equipment. Check that gases are working and adjust air pressure and dampers as follows to ensure proper system operation. The pressure reducing stations are located at the end opposite the baghouse on the skid and include air to the baghouse, aeration, and two pressure reducing stations for the burner unit. The bughouse pressure reducing station should be set to 80 psi (but this will keep on changing during the course of the test). The baghouse should only be used when the pressure differential is greater than $-3 in H_2O$. Also, the air flow to the aeration pads should be 5 cfm at 10-15 psig. The aeration pad adjustment is turned to 0, and the hopper is covered before turning on the aeration pads. The on/off switch is located near the flow adjustment for the aeration pads. The valve for the air supply to the air slide is open.

4. Connect the Fluke data logger to the laptop and to the thermocouples.
5. Turn on water supply (two connections) to cool the equipment in order to prevent overheating. The water level in the scrubber should never reach the top of the sight glass, but should be maintained at center of the sight glass. If water levels move too high, adjust the flow out of the scrubber and if necessary adjust the water inflow valve to maintain desired levels. Water draining from the scrubber should be collected in a bucket.
6. It should be ensured that air has been turned on for at least two minutes before attempting to start or restart the burner. If the burner trips, wait two minutes for the system to purge and press reset button. Connect the burner scanner to the burner. Turn on gas, gas valve, and ignite by plugging it in and pressing the red button on the side of the safeguard system. The burner will start itself (and trip out if it does not detect flame within 10 seconds). Set the burner controller (located near the rotary feeder) in manual and set it to 25%. Allow 5 minutes for the system to warm up and equilibrium to occur then set the burner controller to automatic. The temperature will initially be set to 1000^{o}F at the inlet of the air slide, but the set point can also be adjusted by using the control pad.
7. Use caution when placing the test sample into the feed hopper. Place feed material (virgin PAC/TOXECON) into feed hopper by transferring material into a 5 gallon pail and pouring it into the hopper. Secure cover firmly onto the feed hopper.
8. Open gate (all the way to the top) at the end of the air slide. Set the feeder to 1200 rpm. Monitor system temperatures and pressures and adjust automated burner controls as necessary. Over the course of the test, the pressure in the unit will remain at 1-3 psig at

the air slide inlet. The temperature for the burner unit depends on the monitoring area. During operation, the baghouse will need to be pulsed (by turning the controller to "On") if it reaches a pressure differential of –2 to –3 inH_2O. Monitor the material flow from the hopper. It is important to wear safety goggles and a dust mask or respirator when doing this.

9. Continue operations until feed material is gone.

Shut-Down Procedures:

10. Close slide gate and turn off rotary feeder. Leave heat on for additional five minutes to ensure complete material run is completed.
11. Turn off heat (shut off gas and pull plug) and allow air to purge system for additional 30 minutes or until the system cools down and temperatures reach a safe level.
12. Close the valve supplying air to the air slide, and then open the gate valve below the baghouse. Pulses the baghouse at five-minute intervals during cooling to make sure that the bags are properly purged.
13. Turn off water and air, and disconnect power lines. Place a baggie over the gas line connection to ensure that no foreign material enters this line while it is shutdown. Remove the burner scanner and place it in the scanner box to ensure that it is protected.
14. Allow the product material drum (underneath the air slide) to cool down.

APPENDIX B

SEM IMAGES AND ENERGY DISPERSIVE X-RAY ANALYSIS ON PAC SAMPLES FROM THE TOXECON™ PROCESS

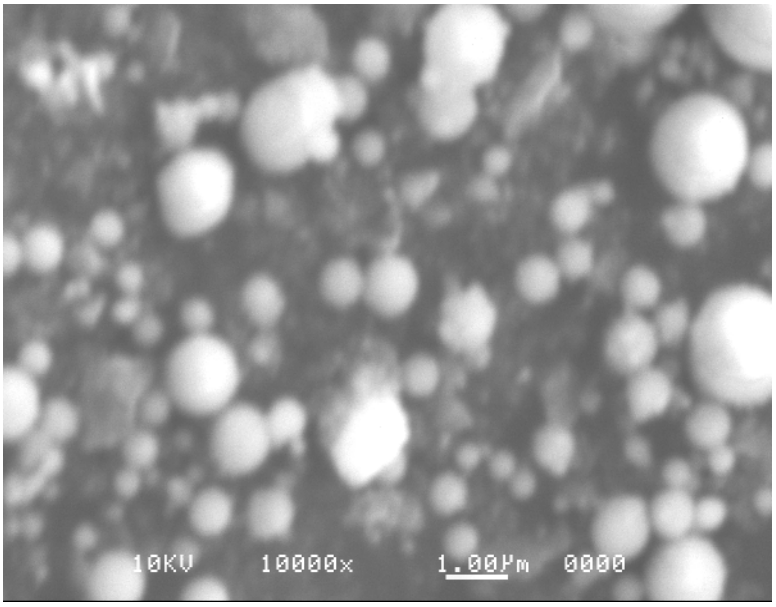

SEM image of PAC sample from the TOXECON process as delivered (X10000)

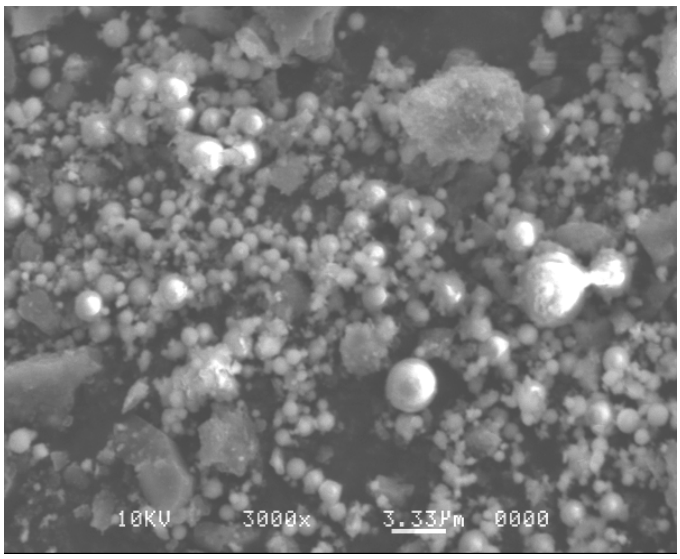

SEM image of PAC sample from the TOXECON process after thermal treatment at 1000°F for 2 hrs in an inert atmosphere the TGA (X3000)

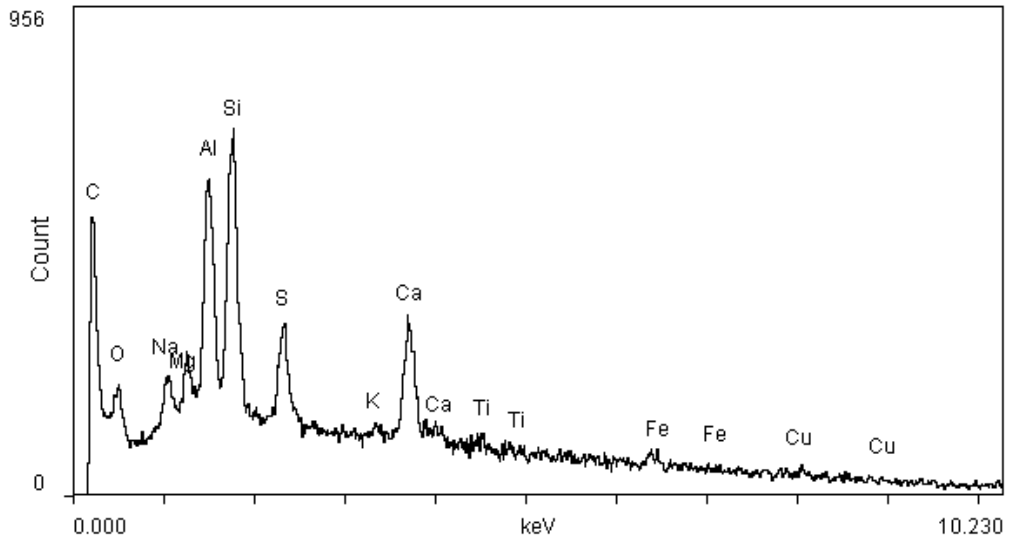

Energy Dispersive X-ray analysis of a coarse PAC particle as delivered (X500)

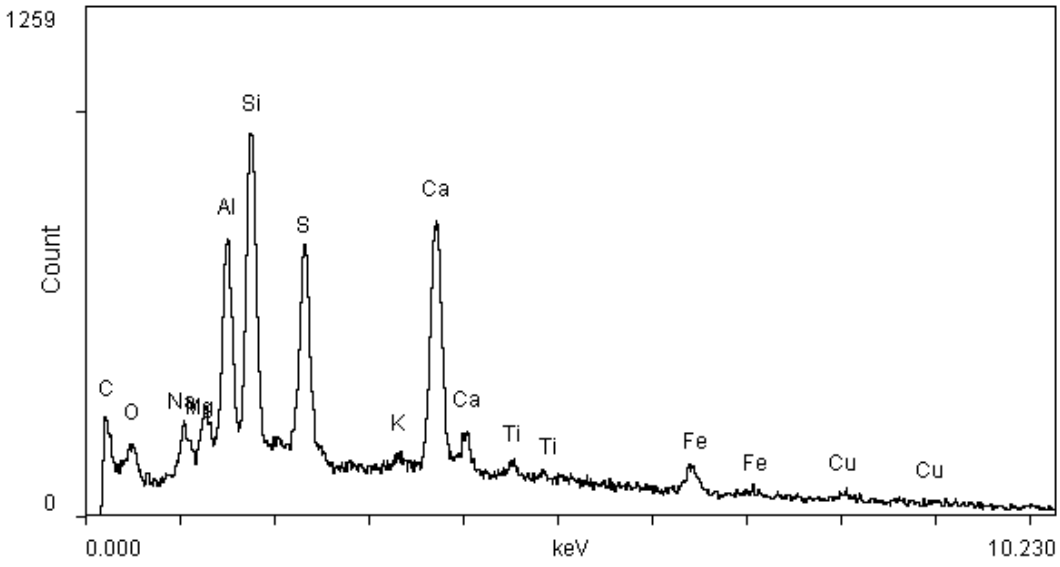

Energy Dispersive X-ray analysis of an average PAC sample area as delivered (X500)

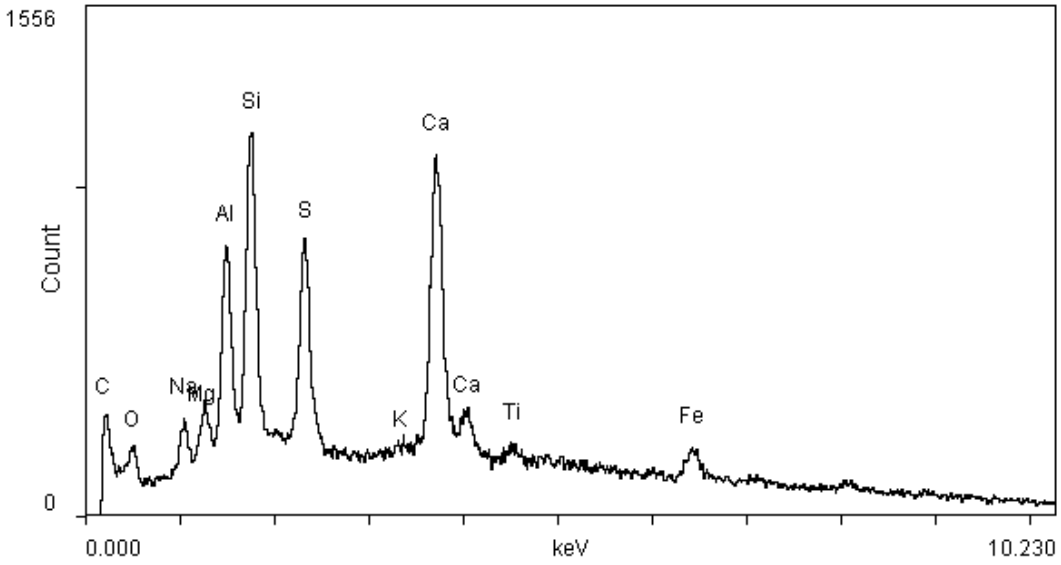

Energy Dispersive X-ray analysis of an average PAC sample area after thermal treatment at 700^{o}F for 2 hrs in the TGA (X500)

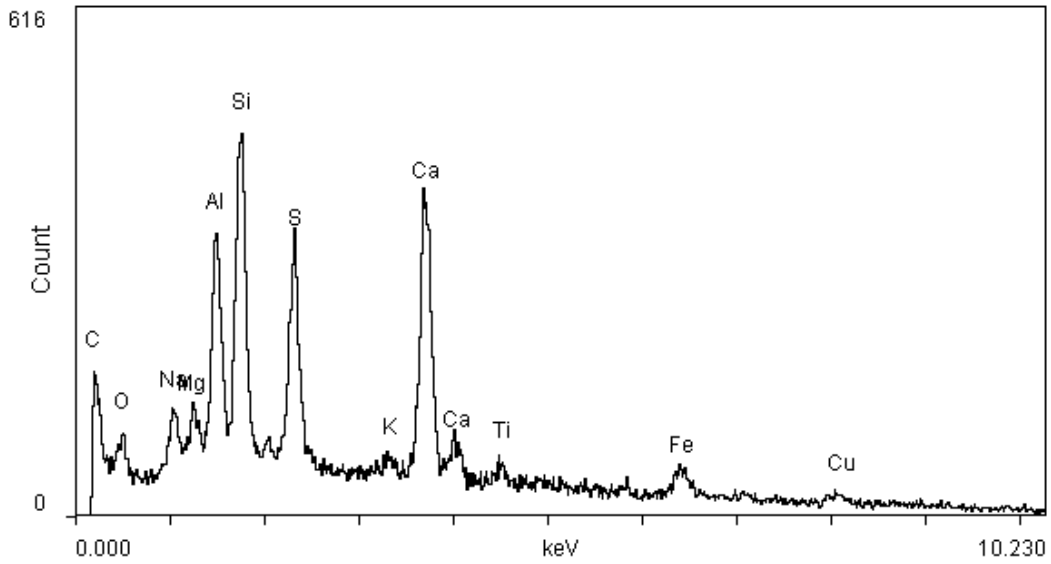

Energy Dispersive X-ray analysis of an average PAC sample area after thermal treatment at 800^{o}F for 2 hrs in an inert atmosphere in the TGA (X500)

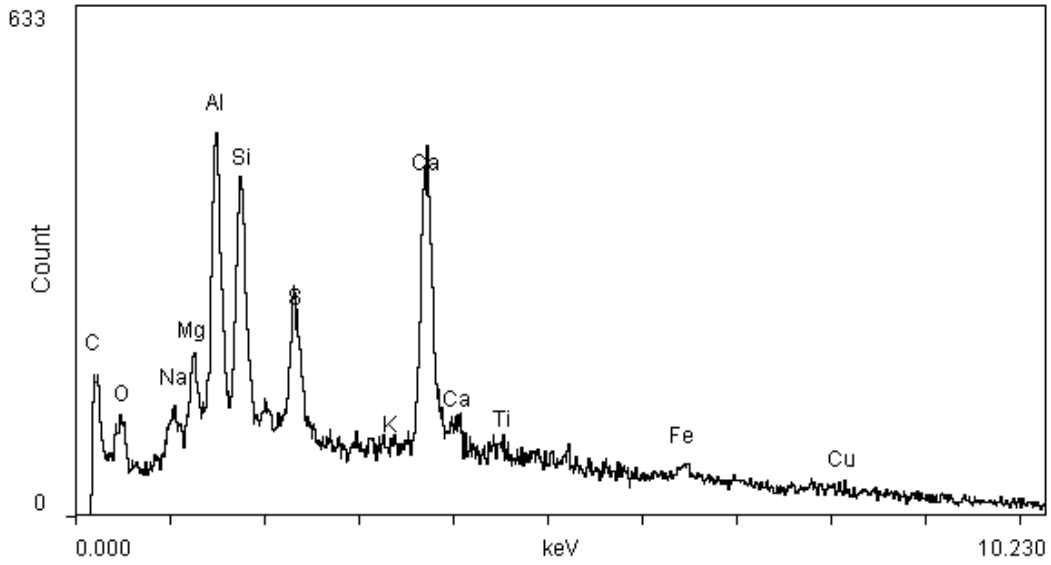

Energy Dispersive X-ray analysis of fine PAC particle after thermal treatment at 1000^{o}F for 2 hrs in an inert atmosphere in the TGA (X500)

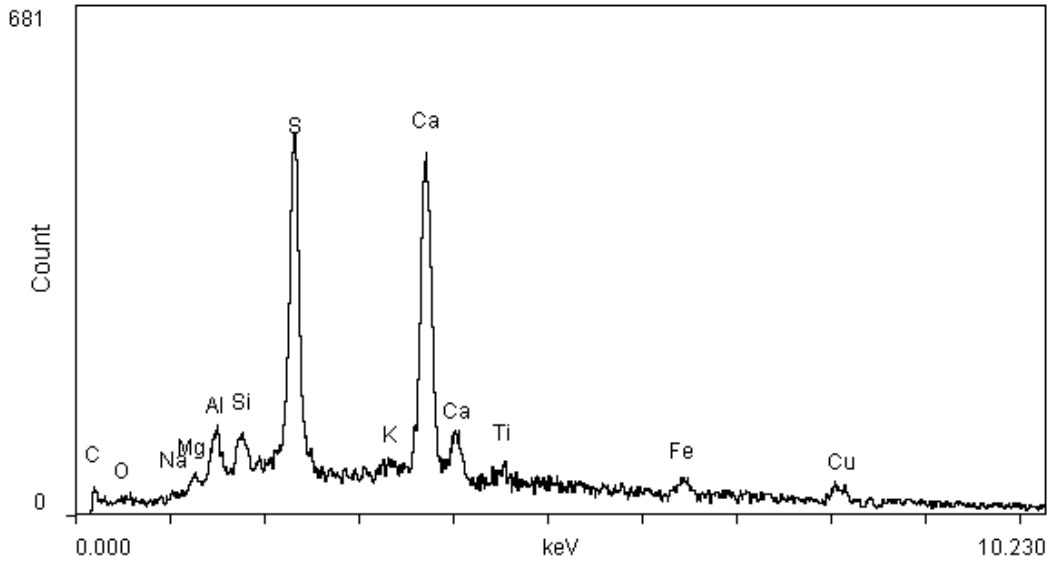

Energy Dispersive X-ray analysis of a coarse PAC particle after addition of a mixture of 1%CuO+4%Fe_2O_3 catalyst and heated at 900^{o}F for 2 hrs in an inert atmosphere in the TGA (X500)

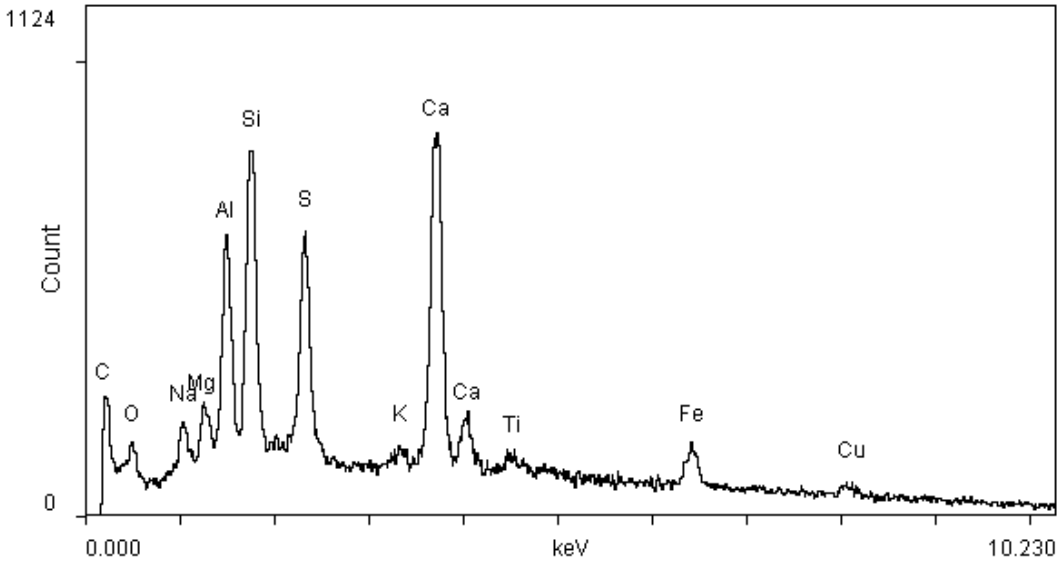

Energy Dispersive X-ray analysis of an average PAC sample area after addition of a mixture of 1%CuO+4%Fe_2O_3 catalyst and heated at 900^oF for 2 hrs in an inert atmosphere in the TGA (X500)

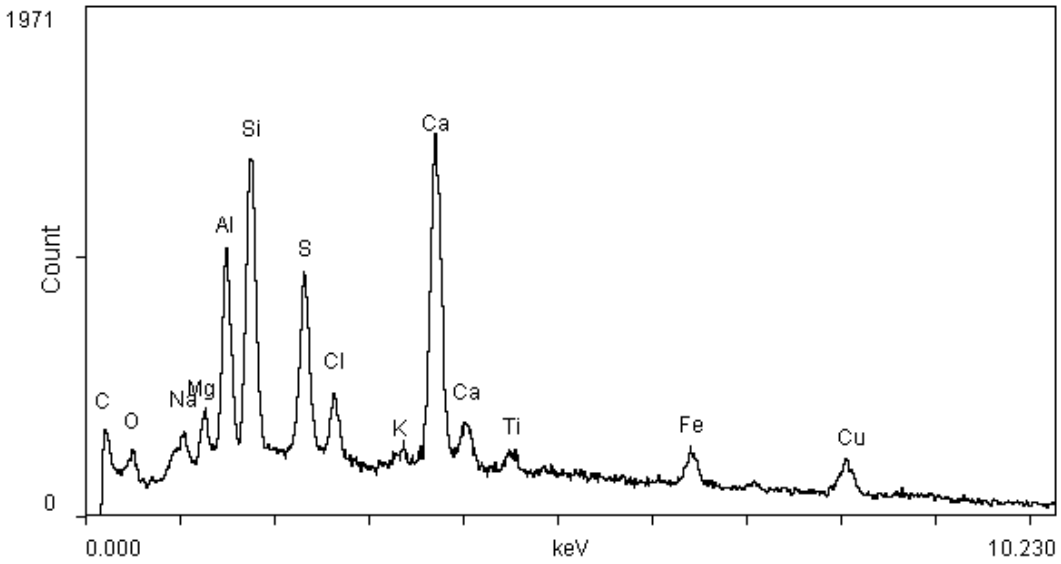

Energy Dispersive X-ray analysis of an average PAC sample area after addition of 5% CuCl catalyst and heated at 700^oF for 2 hrs in an inert atmosphere in the TGA (X500)

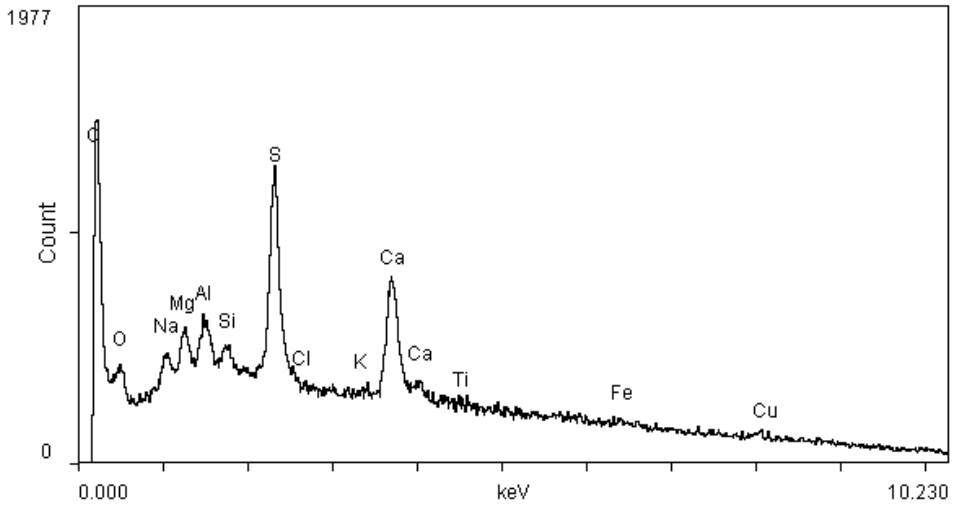

Energy Dispersive X-ray analysis of a coarse PAC particle after thermal treatment at 1200^{o}F for 3-4 min. in the Air Slide bed (X500)

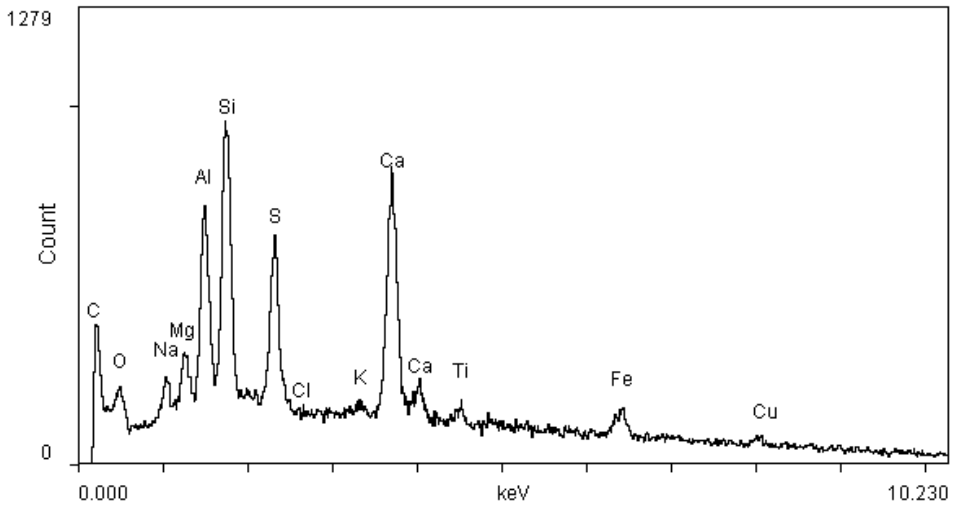

Energy Dispersive X-ray analysis of an average PAC sample area after thermal treatment at 1200^{o}F for 3-4 min. in the Air Slide bed (X500)

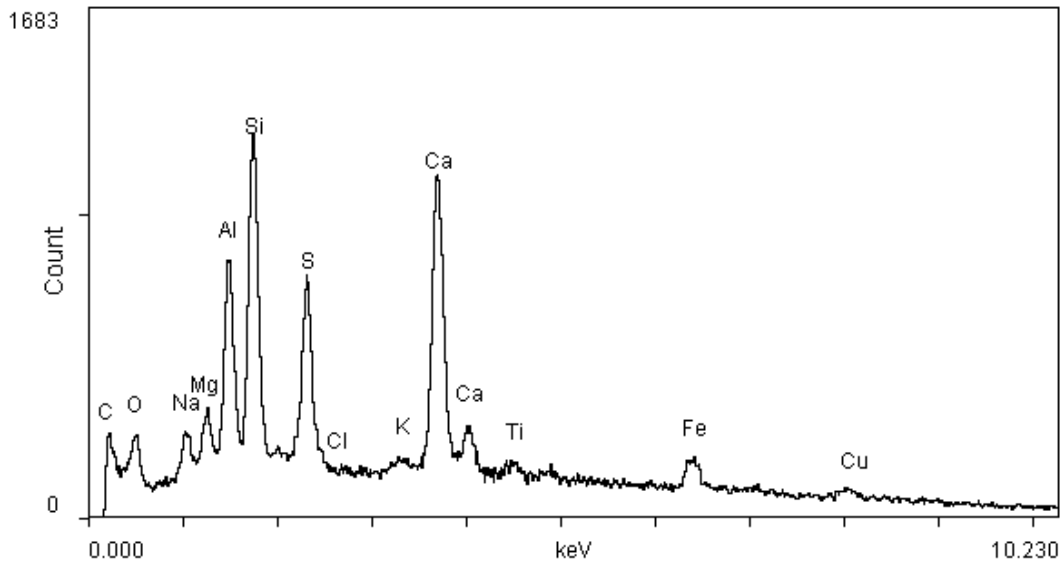

Energy Dispersive X-ray analysis of an average PAC sample area after thermal treatment at 1200^{o}F for 3-4 min. in the Air Slide (baghouse) (X500)

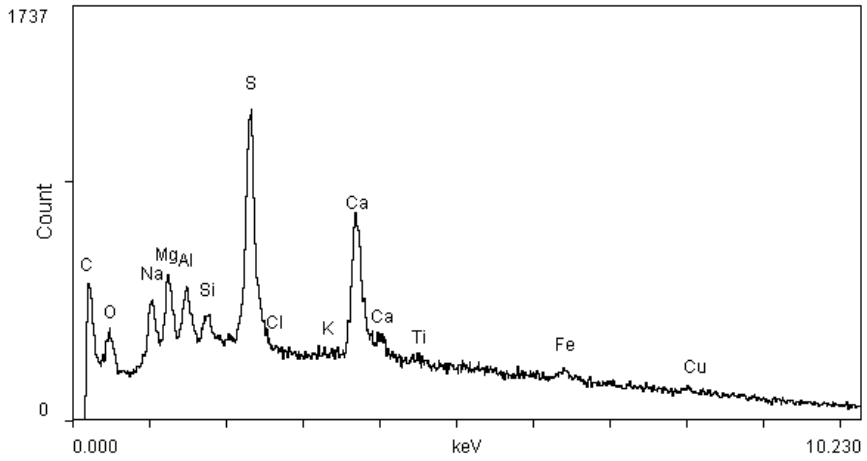

Energy Dispersive X-ray analysis of a coarse PAC particle after thermal treatment at 1200^{o}F for 3-4 min. in the Air Slide (baghouse) (X500)

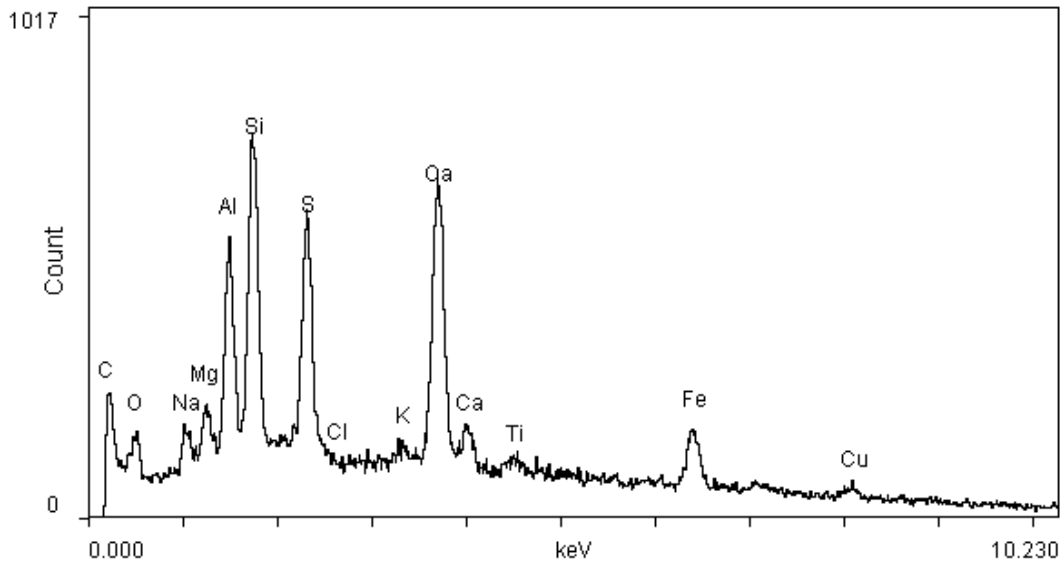

Energy Dispersive X-ray analysis of an average PAC sample area after addition of a mixture of 1%CuO+4%Fe_2O_3 catalyst and heated at 700^{o}F for 3-4 min. in the Air Slide bed (X500)

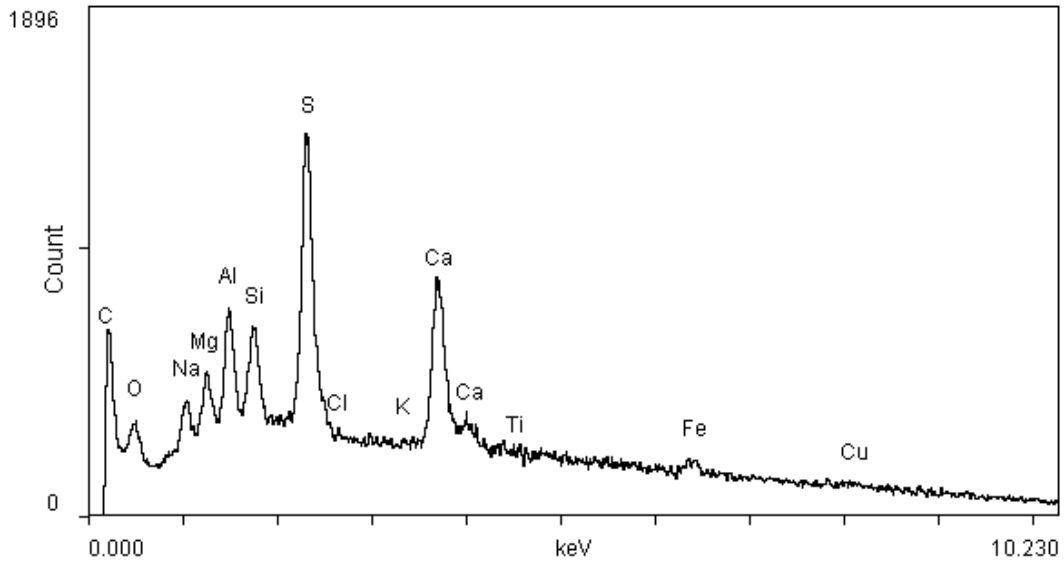

Energy Dispersive X-ray analysis of a coarse PAC sample after addition of a mixture of 1%CuO+4%Fe_2O_3 catalyst and heated at 700^{o}F for 3-4 min. in the Air Slide (baghouse) (X500)

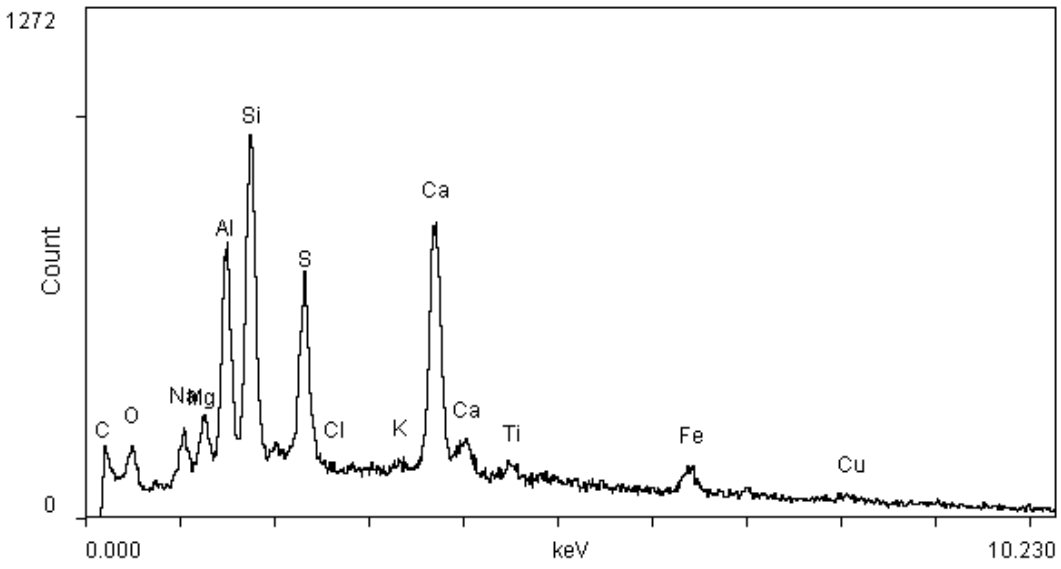

Energy Dispersive X-ray analysis of an average PAC sample area after addition of a mixture of 1%CuO+4%Fe_2O_3 catalyst and heated at 700^oF for 3-4 min. in the Air Slide (baghouse) (X500)